STRUCTURAL SCIENCE
CRYSTAL ENGINEERING
MATERIALS

Volume 81 (2025)

Supporting information for article:

Quantitative crystal structure analysis in trifluoromethyl- and cyano-substituted *N*-phenylbenzamides

Koushik Mandal and Deepak Chopra

S1. Synthesis

S2. Characterization

S2.1. NMR spectroscopy

S2.2. Differential scanning calorimetry (DSC)

S2.3. Crystallization experiments and crystal screening for polymorphism

S2.4. Single crystal X-ray diffraction (SCXRD)

S2.5. Powder X-ray diffraction (PXRD)

S3. Geometrical parameters, interaction topology and table of intermolecular interactions

S4. Hirshfeld surface analysis and 2D-Finger print plots

S5. Lattice energy

S6. Polymorph prediction

S1. Synthesis

The -CN and -CF_3 substituted benzamides have been synthesized by nucleophilic substitution reaction wherein the -CN substituted anilines and DMAP act as a nucleophile and base, respectively. In a round bottomed flask, 10 ml of dry dichloromethane was added, to which aniline and DMAP were added in a 1:1.2 equimolar ratio and the solution was stirred for 0.5h at 0-5ºC on a magnetic stirrer under an inert atmosphere. Subsequent addition of -CF_3 substituted benzoyl chlorides with stirring for 16 hours at room temperature yields the respective substituted benzanilides. The completion of the reaction was monitored using thin-layer chromatography. The quenching of the reaction was carried out using 10% hydrochloric acid. It was dried using sodium sulfate and finally purified by column chromatography. The products have been characterized through NMR and further crystallized using a library of solvents [dichloromethane, toluene, chloroform, nitromethane, dioxane, hexane, DCM-hexane, methanol, isopropanol, acetone, acetonitrile, ethyl acetate].

S2. Characterization

S2.1. NMR

^{1}H-NMR spectra of substituted benzamides were collected using $CDCl_3$ solvent where all the protons including amide protons lie within the aromatic regions of 7.26-8.54 *ppm* (Fig. S1).

(a) N-(2-cyanophenyl)-2-(trifluoromethyl) benzamide (2CN2T): ^{1}H NMR (400 MHz, Chloroform-*d*) δ 8.54 (d, *J* = 8.5 Hz, 1H), 7.95 (s, 1H), 7.81 (d, *J* = 7.5 Hz, 1H), 7.68 (dt, *J* = 18.7, 6.0 Hz, 5H), 7.32 – 7.26 (m, 1H).

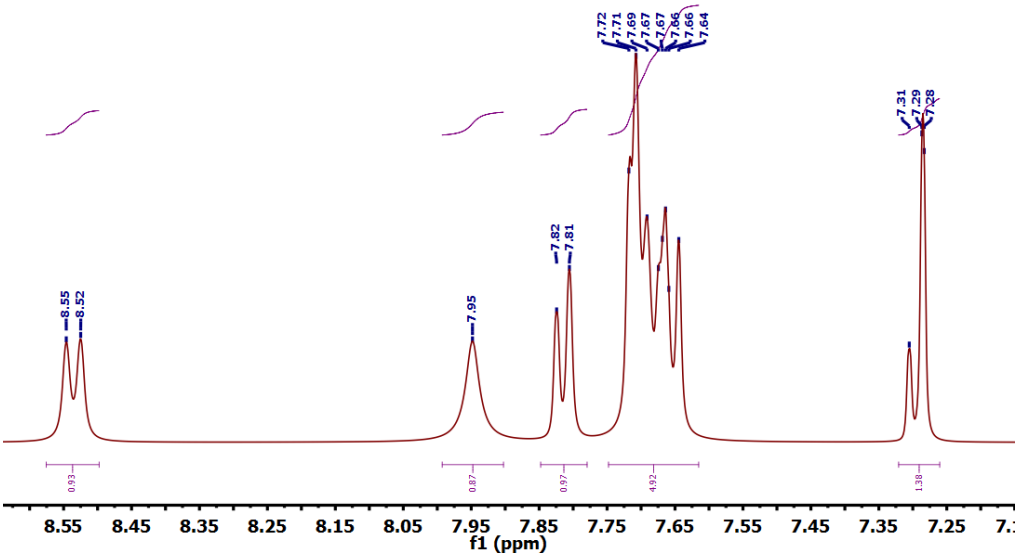

(b) N-(2-cyanophenyl)-3-(trifluoromethyl) benzamide (2CN3T): ^{1}H NMR (400 MHz, Chloroform-*d*) δ 8.58 (d, *J* = 8.4 Hz, 1H), 8.39 (s, 1H), 8.27 (d, *J* = 2.2 Hz, 1H), 8.11 (d, *J* = 7.8 Hz, 1H), 8.00 – 7.87 (m, 1H), 7.74 – 7.66 (m, 3H), 7.33 – 7.26 (m, 1H).

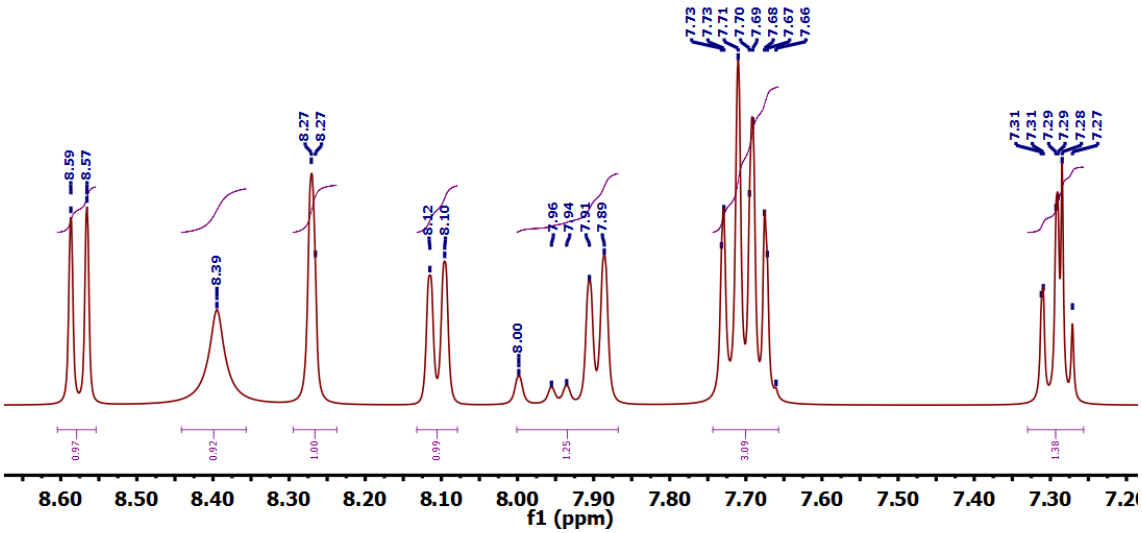

(c) N-(2-cyanophenyl)-4-(trifluoromethyl) benzamide (2CN4T): ^{1}H NMR (400 MHz, Chloroform-*d*) δ 8.59 (d, *J* = 8.4 Hz, 1H), 8.42 (s, 1H), 8.08 (d, *J* = 8.0 Hz, 2H), 7.83 (d, *J* = 8.0 Hz, 2H), 7.74 – 7.64 (m, 2H), 7.32 – 7.27 (m, 1H).

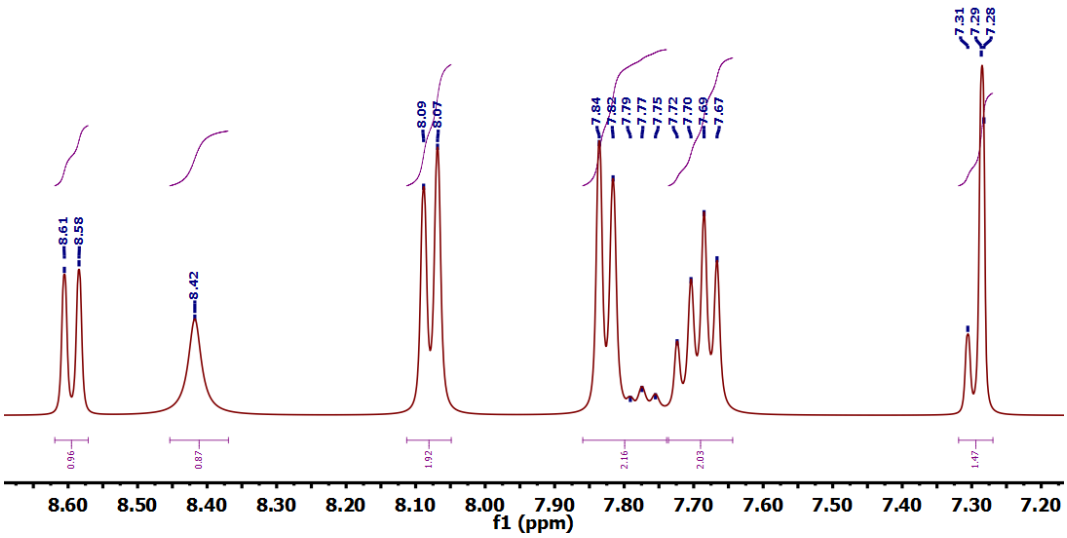

(d) N-(3-cyanophenyl)-2-(trifluoromethyl) benzamide (3CN2T): ^{1}H NMR (400 MHz, Chloroform-*d*) δ 8.02 (d, *J* = 2.1 Hz, 1H), 7.81 (ddd, *J* = 7.6, 4.9, 2.6 Hz, 2H), 7.73 – 7.62 (m, 4H), 7.53 – 7.46 (m, 2H).

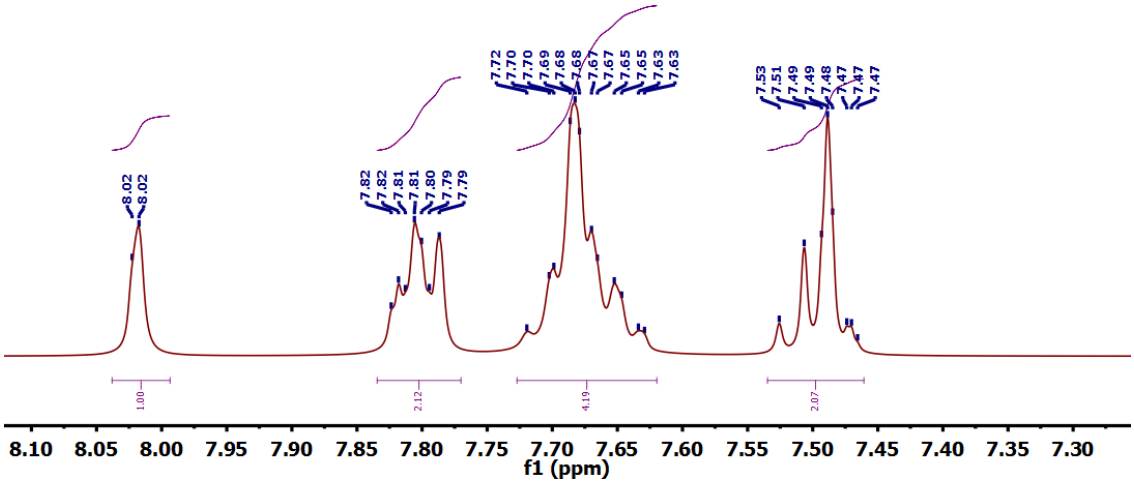

(e) N-(3-cyanophenyl)-3-(trifluoromethyl) benzamide (3CN3T): ^{1}H NMR (400 MHz, Chloroform-*d*) δ 8.15 (d, *J* = 1.8 Hz, 1H), 8.13 – 8.07 (m, 3H), 7.94 – 7.85 (m, 2H), 7.69 (t, *J* = 7.8 Hz, 1H), 7.56 – 7.46 (m, 2H).

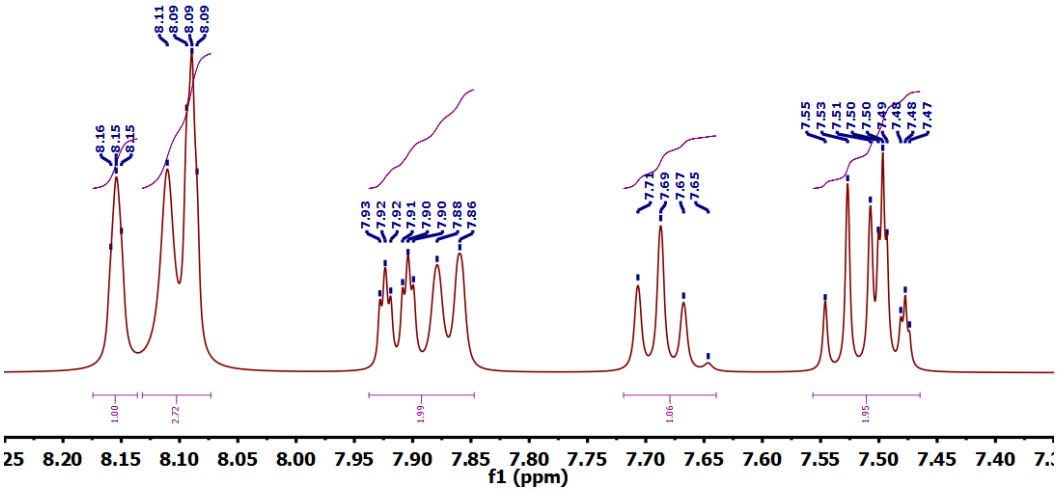

(f) N-(3-cyanophenyl)-4-(trifluoromethyl) benzamide (3CN4T): ^{1}H NMR (400 MHz, Chloroform-*d*) δ 8.09 (s, 1H), 8.00 (t, *J* = 10.6 Hz, 3H), 7.85 (dd, *J* = 30.1, 7.9 Hz, 3H), 7.57 – 7.47 (m, 2H).

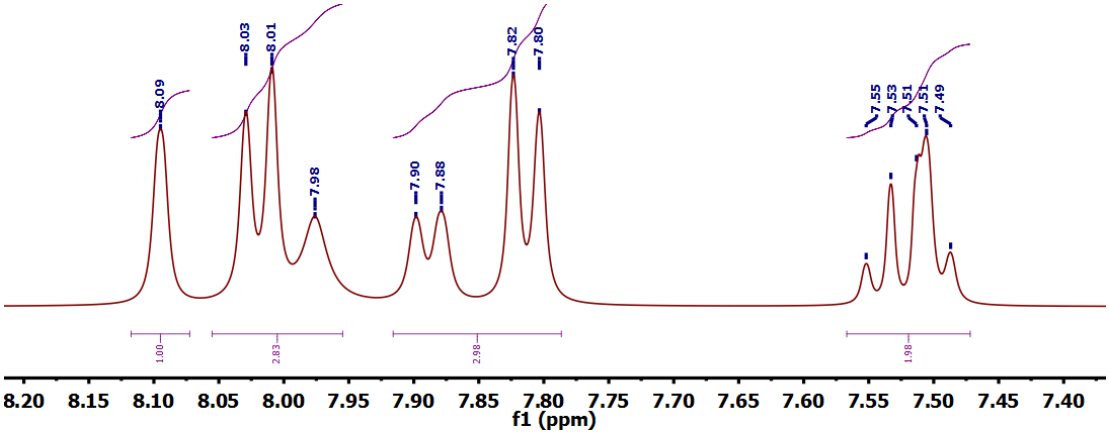

(g) N-(4-cyanophenyl)-2-(trifluoromethyl) benzamide (4CN2T): ^{1}H NMR (500 MHz, Chloroform-d) δ 7.79 (d, J = 7.7 Hz, 2H), 7.75 (d, J = 8.4 Hz, 2H), 7.71 – 7.63 (m, 5H)

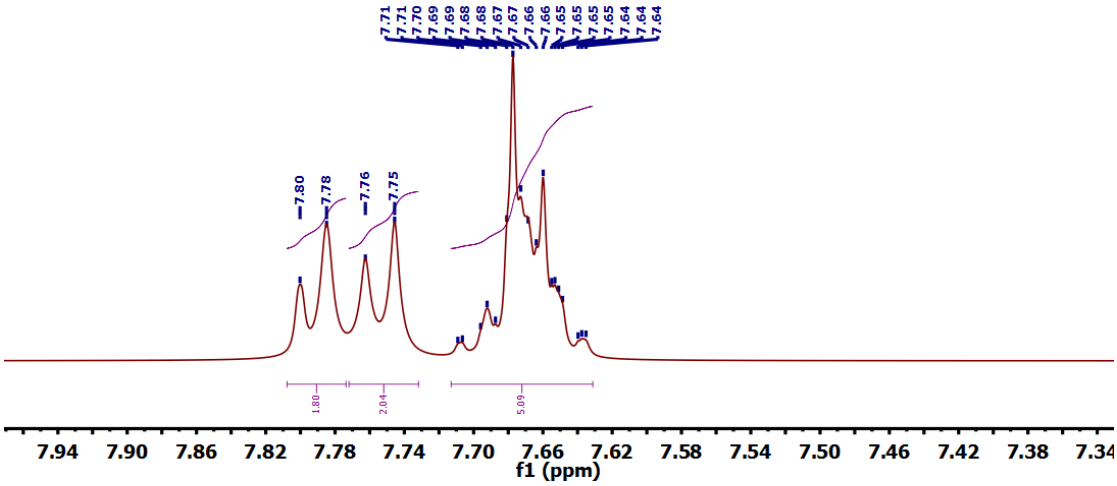

(h) N-(4-cyanophenyl)-3-(trifluoromethyl) benzamide (4CN3T): ^{1}H NMR (400 MHz, Chloroform-*d*) δ 8.16 (s, 1H), 8.12 (d, *J* = 8.0 Hz, 1H), 7.86 (d, *J* = 7.8 Hz, 3H), 7.70 (d, *J* = 8.7 Hz, 2H), 7.29 (d, *J* = 1.2 Hz, 2H).

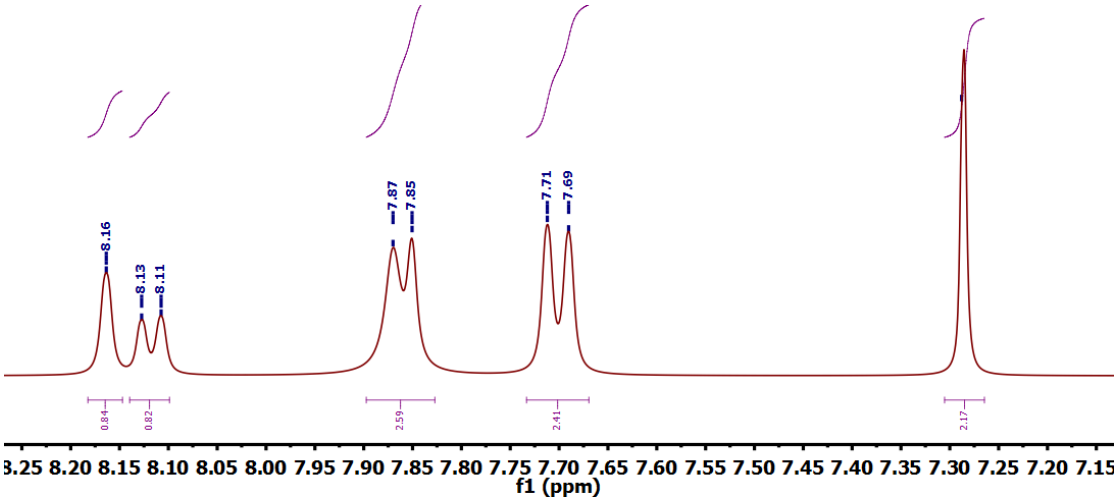

(i) **N-(4-cyanophenyl)-4-(trifluoromethyl) benzamide (4CN4T):** ^{1}H NMR (400 MHz, Chloroform-*d*) δ 8.16 (s, 1H), 8.01 (d, *J* = 8.0 Hz, 2H), 7.87 – 7.77 (m, 3H), 7.69 (dd, *J* = 8.6, 1.5 Hz, 2H), 7.29 (s, 1H).

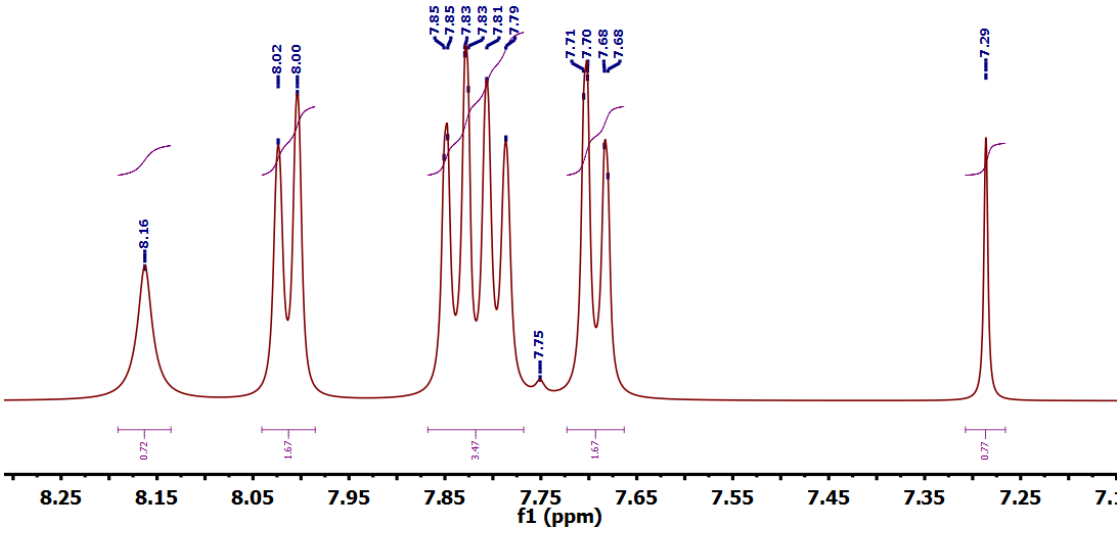

Figure S1. ^{1}H-NMR spectra of (a) 2CN2T, (b) 2CN3T, (c) 2CN4T, (d) 3CN2T, (e) 3CN3T, (f) 3CN4T, (g) 4CN2T, (h) 4CN3T, and (i) 4CN4T respectively.

S2.2. Thermal Characterization

Differential Scanning Calorimetry (DSC). DSC traces of all the synthesized compounds were recorded (**Figs. S2 and S3**) using the Perkin Elmer 6000 DSC instrument. In the case of 4CN4T, due to the appearance of two polymorphic forms (4CN4T.FI and 4CN4T.F2 respectively), DSC traces were recorded in crystals with two different morphologies. In the case of *ortho*-cyano derivatives, 2CN2T has lower thermal stability (122.0°C) whereas 2CN3T has higher thermal stability (194.4°C). In the case of *meta*-cyano derivatives, 3CN2T has lower thermal stability (137.8°C) and 3CN3T has higher thermal stability (189.4°C). In the case of *para*-cyano derivatives, 4CN4T has lower thermal stability (4CN4T.F1 has lower thermal stability (151.4°C) than 4CN4T.F2 , the melting point being157.6°C) and 4CN2T has higher thermal stability (191.2°C). Overall, in the whole series, 2CN4T has the highest melting point and 2CN3T has the lowest melting point.

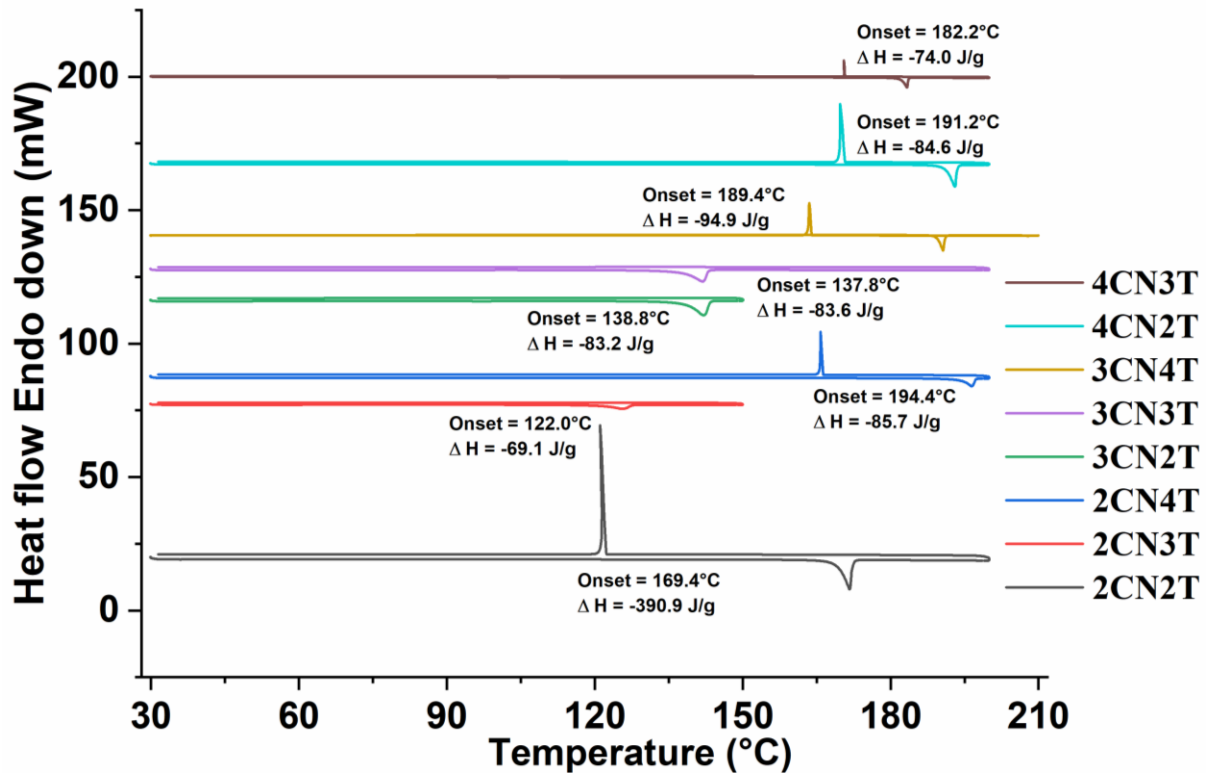

Figure S2: DSC traces for -CN and -CF_3 substituted N-phenyl benzamides.

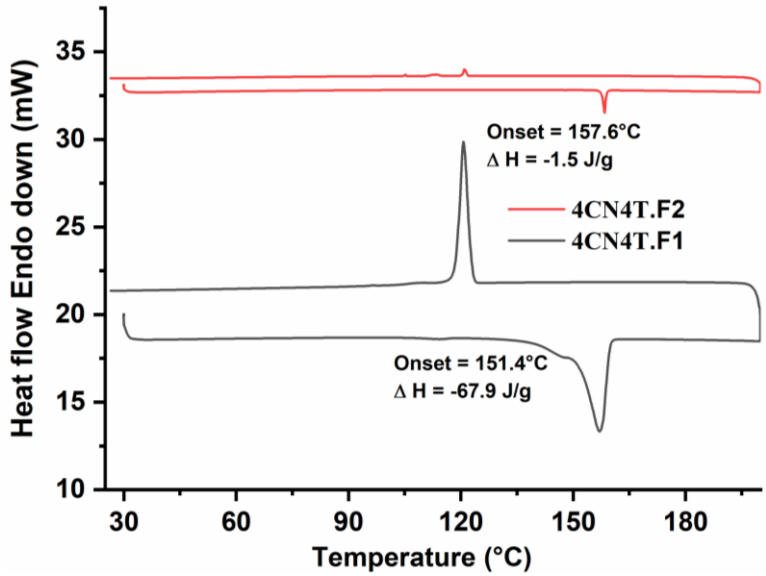

Figure S3: DSC traces for the two concomitant polymorphs of 4CN4T.

S2.3. Crystallization experiments.

All the newly synthesized substituted bulk compounds were kept for crystallization at low temperatures (4°C) and room temperature (27-30°C) using various single and bicomponent organic solvent mixtures. ~4-5 mg of sample was used for each case for crystallization and various methods such as slow evaporation, vacuum sublimation, and melt crystallization were used to screen polymorphs. Among different crystallization methods, slow evaporation was the best method to grow suitable quality single crystals. The results have been tabulated in **Table S1.**

Further extensive crystal screening (obtained via the above-mentioned crystallization methods) was performed to find out the new polymorphic forms, resulting in only one polymorphic form of 4CN4T being observed (Table S3).

Table S1: Crystallization of bulk compounds in various organic solvents and solvent mixtures.

Solvents	Compound code				
	2CN2T	2CN3T	2CN4T	3CN2T	3CN3T
DCM	Plate	Fibrous	Plate	Needle	Block
Methanol	Plate	Needle	Plate	Needle	Block
$CHCl_3$	plate	Fibrous	Fibrous	Needle	Block
Acetonitrile	Needle	Needle	Powder	Needle	Block
DCM+Ethanol	Aggregate	Fibrous	Fibrous	Needle	Block
Nitromethane	Aggregates	Needle	Powder	Needle	Block
THF	Plate	Fibrous	Plate	Powder	Block
Isopropanol	Long plate	Aggregate	Powder	Powder	Powder
EtOAc	Plate	Powder	Aggregate	Needle	Fibrous
DCM+Hexane	Aggregate	Aggregate	Plate	Fibrous	Powder
Acetone	Fibrous	Powder	Aggregate	Aggregate	Fibrous
Dioxan	Fibrous	Aggregate	Powder	Needle	Fibrous
DMF	Aggregate	Aggregate	Aggregate	Aggregate	Aggregate
DMSO	Aggregate	Needle	Aggregate	Fibrous	Aggregate

Solvents	Compound code			
	3CN4T	4CN2T	4CN3T	4CN4T
DCM	Rod	Long Plate	Thin Needle	Needle
Methanol	Aggregate	Long Plate	Fibrous	Needle + Block
$CHCl_3$	Aggregate	Aggregate	Fibrous	Needle
Acetonitrile	Needle	Aggregate	Fibrous	Needle
DCM+Ethanol	Fibrous	Long Plate	Fibrous	Needle
Nitromethane	Aggregate	Long Plate	Powder	Needle
THF	Aggregate	Aggregate	Powder	Needle
Isopropanol	Needle	Aggregate	Thin Needle	Aggregate

EtOAc	Rod	Needle	Powder	Aggregate
DCM+Hexane	Fibrous	Fibrous	Aggregate	Needle + Block
Acetone	Needle	Long Plate	Aggregate	Aggregate
Dioxan	Powder	Long Plate	Aggregate	Aggregate
DMF	Fibrous	Aggregate	Aggregate	Powder
DMSO	Fibrous	Aggregate	Aggregate	Aggregate

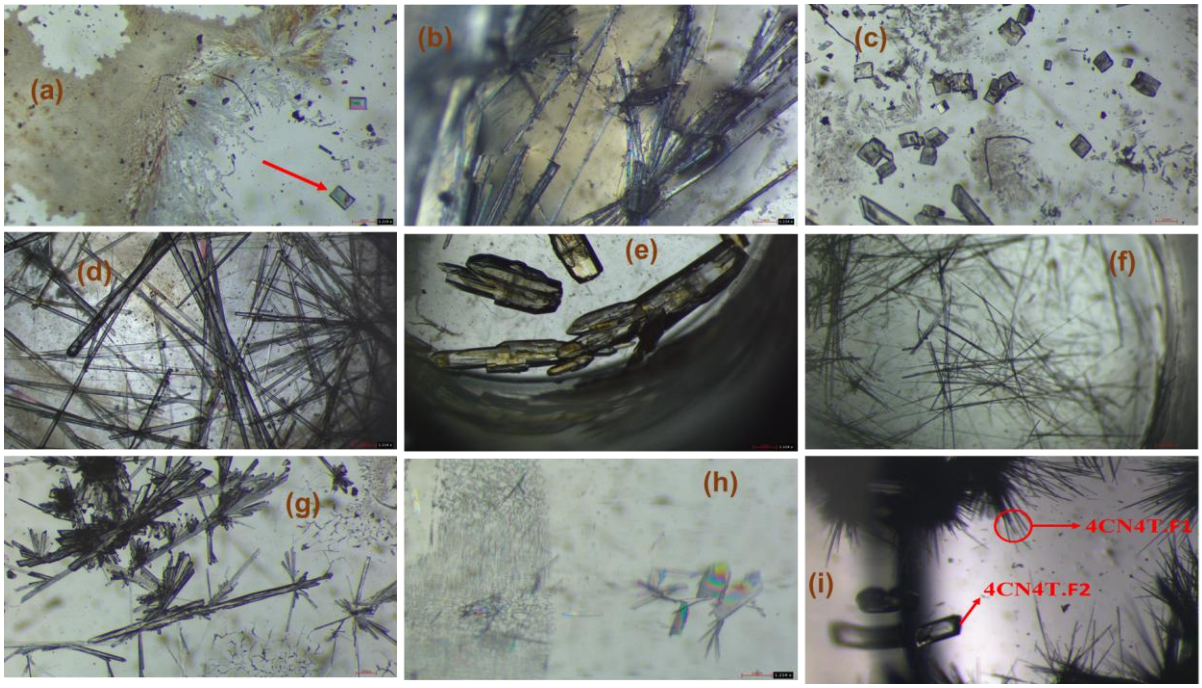

Figure S4. Optical microscopy image of crystals for (a) 2CN2T (b) 2CN3T, (c) 2CN4T, (d) 3CN2T, (e) 3CN3T, (f) 3CN4T, (g) for 4CN2T, (h) 4CN3T, and (i) 4CN4T (F1, F2).

* In each case, the crystal morphology highlighted in red was used further for single-crystal X-ray diffraction (SCXRD).

* In the case of 4CN3T, as no suitable crystals were grown using the slow evaporation method, the vacuum sublimation method resulted in the formation of crystals of long plate morphology suitable for SCXRD.

* Table S1 shows crystals with different morphologies for a particular compound. The crystals not highlighted in red have the same unit cell parameter as the red one.

Table S2. Screening of crystals for polymorphism

Slow evaporation method							
Compound	**Solvent**	**Morphology**	**Result**	**Compound**	**Solvent**	**Morphology**	**Result**
2CN2T	DCM	Plate	2CN2T	2CN3T	Methanol	Needle	2CN3T
	Methanol	Plate	2CN2T		Acetonitrile	Needle	2CN3T
	$CHCl_3$	Plate	2CN2T		Nitromethane	Needle	2CN3T
	Acetonitrile	Needle	2CN2T		DMSO	Needle	2CN3T
	THE	Plate	2CN2T	2CN4T	DCM	Plate	2CN4T
	Isopropanol	Long plate	2CN2T		THF	Plate	2CN4T
	EtOAc	Plate	2CN2T		DCM+Hexane	Plate	2CN4T
3CN2T	DCM	Needle	3CN2T	3CN3T	Methanol	Block	3CN3T
	Methanol	Needle	3CN2T		$CHCl_3$	Block	3CN3T
	$CHCl_3$	Needle	3CN2T		Acetonitrile	Block	3CN3T
	Acetonitrile	Needle	3CN2T		DCM+Ethanol	Block	3CN3T
	DCM+Ethanol	Needle	3CN2T		Nitromethane	Block	3CN3T
	Nitromethane	Needle	3CN2T	4CN3T	DCM	Thin needle	Not diffracted
	Dioxan	Needle	3CN2T		Isopropanol	Thin needle	Not diffracted
	EtOAc	Needle	3CN2T	4CN4T	DCM	Needle	Form I
3CN4T	DCM	Rod	3CN4T		Methanol	Needle+block	Form I+II
	Methanol	Needle	3CN4T		$CHCl_3$	Needle	Form I
	EtOAc	Rod	3CN4T		Acetonitrile	Needle	Form I
	Acetone	Needle	3CN4T		DCM+Ethanol	Needle	Form I
4CN2T	DCM	Long Plate	4CN2T		Nitromethane	Needle	Form I
	Methanol	Long Plate	4CN2T		THF	Needle	Form I
	DCM+Ethanol	Long Plate	4CN2T		DCM+Hex	Needle+block	Form I+II
	Nitromethane	Long Plate	4CN2T				
	Acetone	Long Plate	4CN2T				
	Dioxan	Long Plate	4CN2T				

Sublimation method			**Melt crystallization**		
Com-pound	Morphology	Result	Com-pound	Morphology	Result
2CN2T	Thin plate	2CN2T	2CN2T	Small plate	2CN2T
2CN3T	Thin needle	2CN3T	2CN3T	Thin needle	2CN3T
2CN4T	Long plate	2CN4T	2CN4T	Small plate	2CN4T
3CN2T	Needle	3CN2T	3CN2T	Needle	3CN2T
3CN3T	Tiny block	3CN3T	3CN3T	Block	3CN3T
3CN4T	Thin needle	3CN4T	3CN4T	Very thin eedle	3CN4T
4CN2T	Thin needle	4CN2T	4CN2T	Needle	4CN2T
4CN3T	Long plate	4CN3T	4CN3T	No crystal formed	-
4CN4T	Needle	4CN4T	4CN4T	Needle	4CN4T

***** The results of screening crystals are based on the determination of unit cell.

S2.4. Single-crystal X-ray diffraction (SCXRD):

Crystal data and structure refinement details are summarized in **Table 1**. Single crystal data was collected on the Bruker AXS Kappa APEX II/ Bruker D8 VENTURE (Bruker, 2006) diffractometer using monochromated Mo- Kα radiation (λ = 0.71073 Å). Data reduction was performed *via* Bruker APEX5 v2023.9-0' (Bruker AXS Inc., 2023). The crystal structures were solved by Intrinsic Phasing using the ShelXT program (Sheldrick, 2015*b*, 2008) present in the APEX5. Absorption correction was performed using a multi-scan method implemented in SADABS (Brukar AXS Inc., 2016). All structures were refined by the full-matrix least-squares method using ShelXL 2018, (Sheldrick, 2015*a*) present in the Olex2 interface (Dolomanov *et al.*, 2009). All H atoms, apart from N atom were positioned geometrically and refined using a riding model, with Uiso(H) = 1.2Ueq(C). The crystal packing was generated using Mercury 4.2 (reference in the main manuscript). Geometrical calculations were carried out using PARST (Nardelli, 1995) and PLATON (Spek, 2009).

Structural and refinement details:

The crystal structures of *o*-cyano substituted benzamide molecules such as 2CN2T, 2CN3T, and 2CN4T were refined using the full matrix least squares method using SHELXL 2018. In the case of 2CN2T and 2CN4T, reflections (001) and (020) are the most disagreeable reflections having error/esd value of 24.37 and 19.71 respectively (Most Disagreeable Reflections,

error/esd is calculated as sqrt(wD^2/<wD^2>) where w is given by the weight formula, D = Fo^2-Fc^2 and <> refers to the average over all reflections), and hence have been omitted from the reflection list. In the case of *m*-cyano substituted compounds, such as 3CN2T, 3CN3T, and 3CN4T, the trifluoromethyl group in 3CN3T exhibits rotational disorder with occupancies 0.679(13): 0.321(13). The disorder was treated via the PART instruction. A similar procedure was followed for 4CN3T where both the trifluoromethyl group (Z' = 2) were treated using PART instruction separately and the occupancies were freely refined (0.538(18):0.462(18) for M1; and 0.712(20):0.288(20) for M2). The conformation with the major occupancy was considered further for the analysis of the crystal packing and the calculations on the interaction topology. Also, the two domain twin in 4CN3T was treated by using TWIN/BASF and further HKLF5 command was employed in the last stage of refinement. The BASF value refined to 0.435(7).

S2.5. Powder X-ray Diffraction (PXRD)

~5-8 mg of grounded powder of all the synthesized compounds were used to collect the PXRD data. The bulk compound (EXP powder pattern) and the corresponding simulated powder pattern compound were overlayed to compare the phase purity. Further, *X-pert Highscore plus* software (Degen *et al.*, 2014) was used to quantify the percentage of both phases (4CN4T.F1 and 4CN4T.F2) present in the bulk compound of 4CN4T. It was observed that the bulk compound of 4CN4T more closely corresponds to the 4CN4T.F1 phase (64.8%) than the 4CN4T.F2 (35.2%) (Fig. S5 (j)). Further, profile fitting was performed using *JANA 2020* (Petříček *et al.*, 2023) and the corresponding GOF, Rp, and wRp values are 10.28, 9.67, 16.04 (for 4CN4T bulk and 4CN4T.F1 phase; Fig.S5 (k)) and 20.02, 22.02, 21.24 (for 4CN4T bulk and 4CN4T.F2 phase; Fig. S5 (l)).

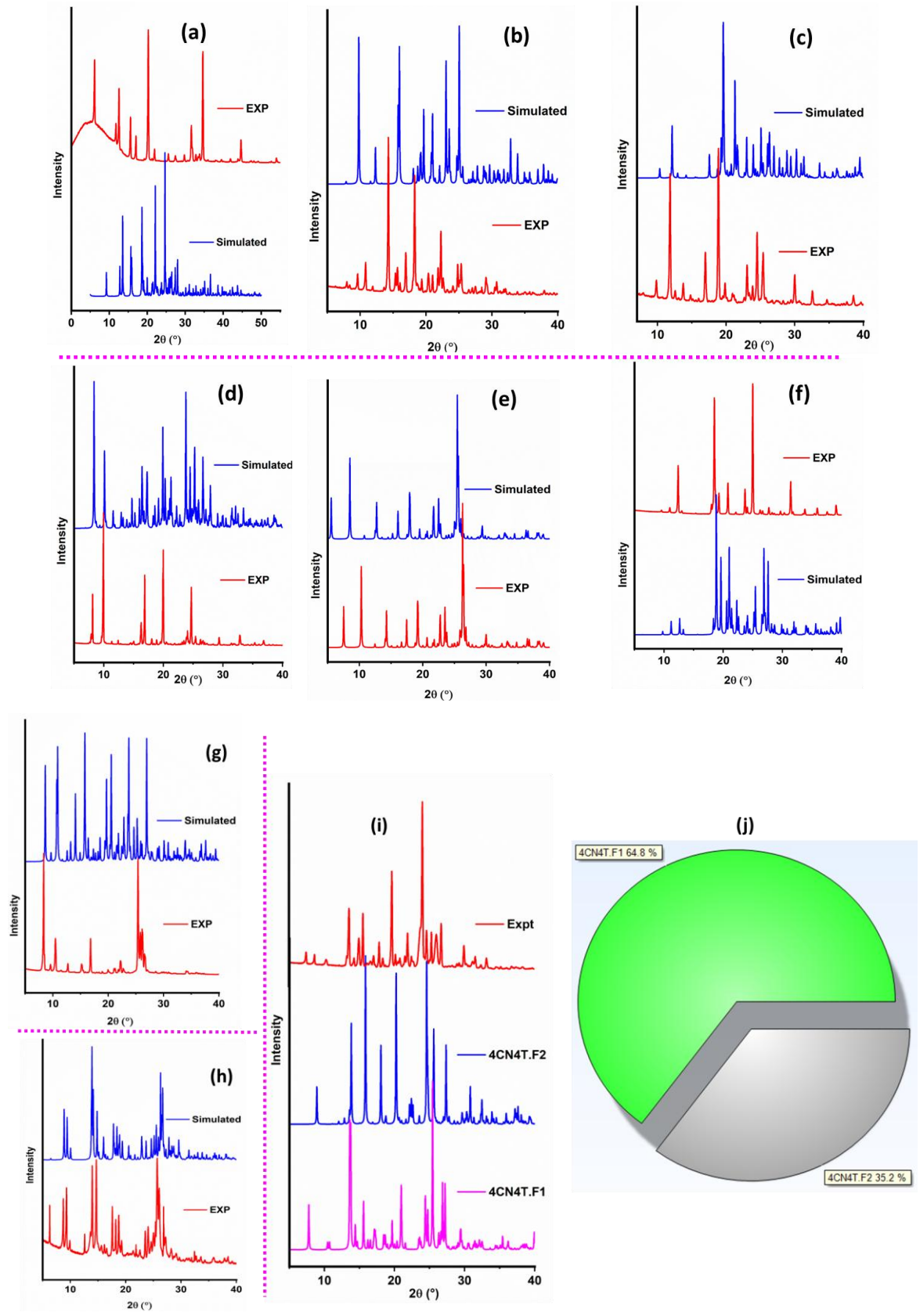
(a)
EXP
Simulated
Intensity
2θ (°)
(b)
Simulated
EXP
Intensity
2θ (°)
(c)
Simulated
EXP
Intensity
2θ (°)
(d)
Simulated
EXP
Intensity
2θ (°)
(e)
Simulated
EXP
Intensity
2θ (°)
(f)
EXP
Simulated
Intensity
2θ (°)
(g)
Simulated
EXP
Intensity
2θ (°)
(h)
Simulated
EXP
Intensity
2θ (°)
(i)
Expt
4CN4T.F2
4CN4T.F1
Intensity
2θ (°)
(j)
4CN4T.F1 64.8 %
4CN4T.F2 35.2 %

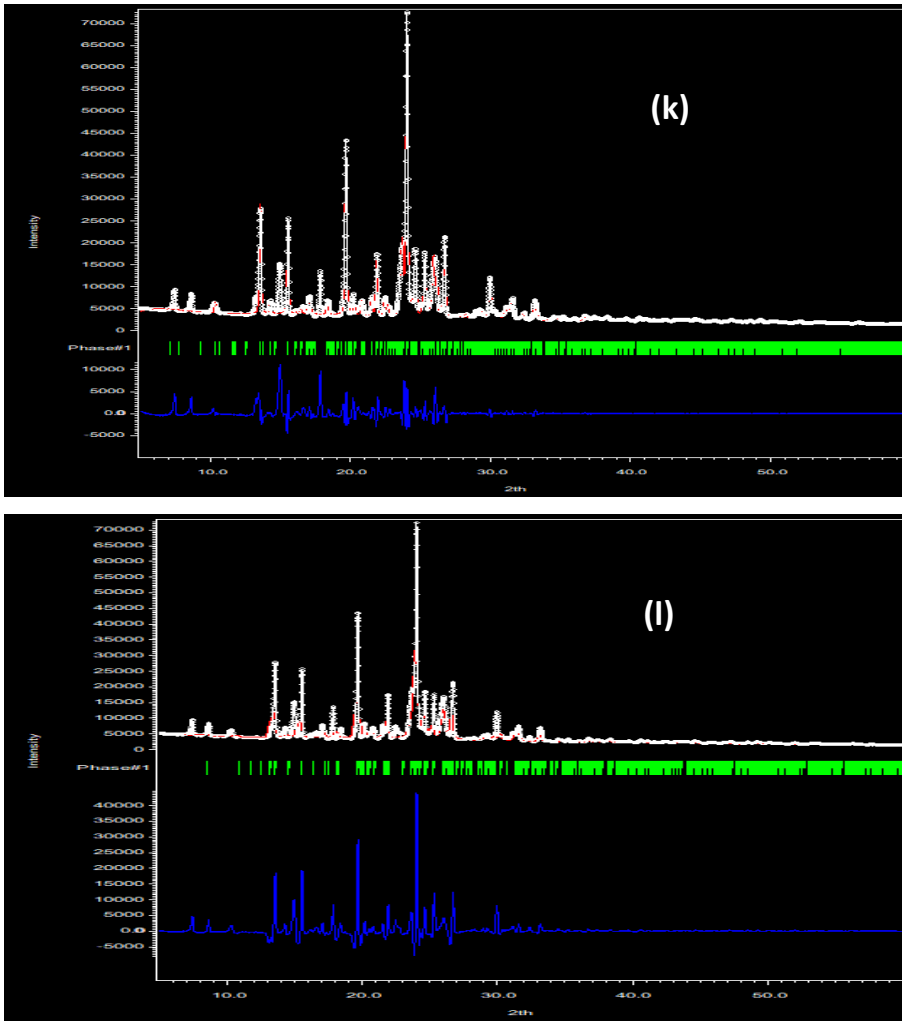

Figure S5. Overlay of the experimental and corresponding simulated powder patterns for (a) 2CN2T (b) 2CN3T, (c) 2CN4T, (d) 3CN2T, (e) 3CN3T, (f) 3CN4T, (g) for 4CN2T, (h) 4CN3T, and (i) 4CN4T, (j) % of phase (4CN4T.F1, and 4CN4T.F2) present in bulk, (k) profile fitting diagram of 4CN4T (experimental) and 4CN4T.F1 (simulated), and (l) profile fitting diagram of 4CN4T (experimental) and 4CN4T.F1 (simulated). In both cases (k, l), the white, red, and blue plot represents the observed, the calculated pattern, and the intensity mismatch between the two powder patterns.

S3. Geometrical Parameters and Interaction Topology:

Crystal packing analysis: The crystal packing analysis has been carried out using Mercury 4.2 [reference in the main manuscript]. The criteria for crystal packing analysis (for 3CN3T, and 4CN3T, the major part of the disorder molecules were considered) are the summation of vdW radii of participating atoms + 0.3Å (Dance, 2003).

Interaction topology and energy decomposition: To visualize the interaction topology associated with the crystal structures (for 3CN3T, and 4CN3T, the major conformer was considered), energy framework analysis has been carried out using *Crystal Explorer 21.5* [reference in the

main manuscript]. The input file was .cif. A 3.8Å cluster was generated and incomplete fragments of the molecules were completed. B3LYP/6-31G(d, p) was used for the calculations to obtain an accurate energy model. The pairwise intermolecular interaction energies in the crystal structures are represented as cylinders joining the molecules. The radii of these cylinders are proportional to the strength of the intermolecular interaction. The tube size was set at the default value of 80, with an energy cut-off of 4 kJ/mol. The values obtained from B3LYP/6-31G (d, p) are scaled for benchmarked energy models using k_ele=1.057, k_pol=0.740, k_disp=0.871, k_rep=0.618. Further % contribution of dispersion energy (%E_{disp}) and electrostatic energy (coulombic+polarization) (%E_{elec}) to the total energy can be calculated using following equation.

$\%E_{disp} = [\frac{Edisp}{Ecol+Epol+Edisp}]\times 100$

$\%E_{elec} = 100 - \%E_{disp}$

Further, Calculation for different motifs present in 2CN2T only are shown below (The values of E_{col}, E_{pol}, and E_{disp} were considered from Table 2) .

Motif I-2, $\%E_{disp} = [\frac{-40.8}{(-36.5)+(-16.5)+(-40.8)}]\times 100 = \sim 43\%$

Motif I-5, $\%E_{disp} = [\frac{-10.4}{(-16.0)+(-4.2)+(-10.4)}]\times 100 = \sim 34\%$

Motif I-8, $\%E_{disp} = [\frac{-10.9}{(-5.2)+(-1.3)+(-10.9)}]\times 100 = \sim 60\%$

Motif I-9, $\%E_{disp} = [\frac{-11.3}{(-3.9)+(-1.1)+(-11.3)}]\times 100 = \sim 69\%$

The same formula was used to get the %E_{disp} of different motifs present in the remaining Compounds from 2CN3T to 4CN4T.F2.

Table S3. List of Intermolecular Interactions. The values of interaction energies and their partitioning were reported in kJ/mol.

Motif	Centroid to centroid distance (Å)	Symmetry code	E_{col}	E_{pol}	E_{disp}	E_{rep}	E_{total}	Possible involved interactions	Geometry (Å/°)
2CN2T									
1 (M2⋯M1)	4.748	x, y, z	-41.8	-20.4	-46.7	58.7	-50.2	N1-H1⋯O2	2.785(2)/1.81/156
2 (M2⋯M1)	5.004	x-1, y-1, z	-36.5	-16.5	-40.8	50.2	-43.6	N3-H3A⋯O1	2.860(2)/1.87/160
								F2⋯π (C24/C25)	3.116(3)/2.961(3)
3 (M2⋯M2)	8.070	x-1, y, z	-19.1	-8.1	-25.6	22.5	-30.3	C28-H28⋯O2	3.673(3)/2.63/463
								C20-H20⋯N4	3.287(4)/2.58/123

								C19-H19···N4	3.289(4)/2.60/121
4 (M1···M1)	8.069	x+1, y, z	-9.9	-6.3	-24.0	16.7	-23.5	C13-H13···F1	3.407(3)/2.60/131
								C5-H5···N2	3.318(4)/2.66/119
5 (M2···M1)	12.044	-x+1, -y, -z+2	-16.0	-4.2	-10.4	11.8	-18.8	C18-H18···N2	3.623(3)/2.56/170
								C3-H3···N4	3.544(3)/2.47/176
6 (M2···M1)	6.883	x, y-1, z	-5.6	-2.3	-24.0	13.4	-18.5	C20-H20···O1	3.658(3)/2.81/135
7 (M2···M2)	7.055	x-1, y, z	-2.9	-2.3	-22.2	10.8	-16.6	C27-H27···F5	3.739(3)/2.79/147
8 (M2···M1)	10.461	-x+1, -y+1, -z+1	-5.2	-1.3	-10.9	4.1	-13.3	C11-H11···F6	3.537(3)/2.83/123
								C26-H26···F3	3.346(3)/2.62/124
								C12-H12···F3	3.410(3)/2.62/129
9 (M2···M1)	10.074	-x, -y, -z+1	-3.9	-1.1	-11.3	5.2	-11.1	C27-H27···F6	3.319(3)/2.70/116
2CN3T									
1	4.934	x-1, y, z	-43.3	-19.4	-51.2	59.1	-54.8	N1-H1···O1	2.867(3)/1.86/165
								C6-H6···O1	3.405(3)/2.73/121
2	6.330	-x+2, -y+1, -z+1	-15.5	-7.9	-40.2	27.5	-36.1	C6-H6···π(C13/C14)	3.577(4)/2.85/135 3.748(4)/2.83/163
3	10.038	-x+2, +y-1/2, -z+1/2	-9.4	-2.8	-9.0	7.4	-13.8	C13-H13···N2	3.380(4)/2.60/128
4	10.818	x-1, -y+1/2+1, +z+1/2	-9.5	-1.9	-3.4	2.4	-12.4	C5-H5···N2	3.835(4)/2.76/173
5	9.486	-x+1, +y+1/2, -z+1/2	-1.7	-0.4	-5.0	0.9	-6.2	F3··· π (C3)	3.394(3)
6	10.098	x+1, -y+1/2+1, +z+1/2	-1.2	-1.6	-9.3	6.8	-5.3	C3-H3···F1	3.556(3)/2.50/166
								C4-H4···F2	3.243(3)/2.52/123
2CN4T									
1	4.987	x+1, y, z	-40.7	-17.5	-46.2	50.6	-53.8	N1-H1···O1	2.879(3)/1.88/162
								C6-H6···O1	3.402(4)/2.72/121
								C15-F2···F1-C15	2.881(3)/157, 129
2	11.383	-x, -y+1, -z+2	-25.7	-7.8	-12.6	19.4	-26.7	C3-H3···N2	3.455(4)/2.40/166
3	7.951	x+1, y, z+1	-11.6	-6.5	-24.0	19.3	-22.8	C4-H4···N2	3.278(3)/2.51/127
								C6-H6··· π (C13)	3.723(4)/2.87/149
4	10.174	x, y, z+1	-0.6	-3.9	-22.7	11.8	-15.4	C10-H10···F2	3.78 6(4)/2.80/152
								C13-H13··· π (C6)	3.671(4)/2.85/145

5	9.467	x-1/2, -y+1/2, +z+1/2	-2.5	-1.0	-7.9	4.5	-6.9	C10-H10···F3	3.314(4)/2.52/130
								C11-H11···F1	3.529(3)/2.67/136
3CN3T									
1	4.312	x, -y+1/2+1, +z+1/2	-56.7	-21.3	-56.2	71.3	-62.9	N1-H1···O1	2.809(2)/1.83/159
								C10-H10···O1	3.400(2)/2.73/120
								C10-H10···F3	3.301(6)/2.48/132
2	10.790	-x+1, +y-1/2, -z+1/2+2	-8.3	-6.0	-21.2	17.2	-18.3	C3-H3···O1	3.409(2)/2.61/130
								C4-H4···N2	3.445(2)/2.60/134
3	7.937	-x+2, -y+2, -z+2	-3.3	-2.1	-29.0	18.4	-16.0	F2···π (C14)	3.162(6)
4	12.576	x, y+1, z	-7.6	-2.5	-5.7	4.8	-11.0	C13-H13···N2	3.485(2)/2.70/129
5	11.354	-x+2, -y+2, -z+1	-5.2	-1.2	-9.7	6.0	-10.1	C12-H12···F3	3.486(5)/2.56/143
6	8.816	-x+2, +y-1/2, -z+1/2+1	-4.3	-2.3	-12.5	9.1	-10.0	C7-H7···F2	3.490(6)/2.44/163
								C13-H13···F1	3.164(7)/2.45/122
3CN4T									
1	9.867	-x+2, -y+1, -z+1	-59.8	-18.4	-29.9	43.6	-64.5	C10-H10···N2	3.5387(2)/2.48/167
								C7-H7···N2	3.4308(1)/2.44/153
								N1-H1···N2	3.4372(2)/2.61/137
2	4.719	x+1, +y, +z	-21.0	-9.6	-42.0	33.6	-39.0	N1-H1···O1	2.8931(3)/2.16/127
3	8.844	-x, -y+2, -z+1	-13.4	-7.8	-23.7	20.7	-24.2	C4-H4···O1	3.2768(3)/2.47/130
4	9.425	-x+1/2+1, +y-1/2, -z+1/2	-3.0	-1.2	-9.9	4.0	-10.2	C11-H11···F3	3.3744(3)/2.54/133
5	8.898	-x+1, -y+1, -z+1	5.8	-5.0	-27.6	16.1	-10.7	N2···π (C8)	3.2234(3)
6	9.208	-x+1/2, +y+1/2, -z+1/2	-2.0	-1.1	-11.2	4.7	-9.7	C13-H13···F2	3.2963(3)/2.65/118
7	14.428	x-1/2, -y+1/2+1, z+1/2	-1.5	-0.4	-4.0	1.2	-4.7	C3-H3···F1	3.7208(1)/2.68/162
								C3-H3···F2	3.4693(1)/2.75/123
								N2···F3	2.9876(1)/114
4CN2T									
1 (M2···M1)	4.914	x+1/2, -y+1/2+1, +z+1/2	-43.1	-18.3	-39.3	50.1	-50.6	N1-H1···O2	2.904(3)/1.88/176
								C4-H4···O2	3.481(4)/2.67/132
								C30-F4···F3-C15	2.817(2)/149, 127
2	7.686					45.0		C29-H29···N4	3.340(5)/2.65/121

(M2···M2)		-x+2, -y+1, -z+1	-28.7	-10.4	-49.9		-44.0	(C18) π···π (C20)	3.360(5)
								C18-H18···O2	3.544(4)/2.77/129
3 (M2···M1)	5.095	x, y, z	-35.6	-17.0	-45.2	54.6	-43.2	N3-H3A···O1	2.866(3)/1.85/168
								F1···π (C25)	3.082(3)
4 (M2···M1)	10.764	-x+1/2+2, +y+1/2, -z+1/2+1	-14.3	-6.0	-16.3	13.7	-22.9	C19-H19···N2	3.489(4)/2.47/156
								C4-H4···N4	3.393(4)/2.56/134
5 (M2···M2)	10.276	-x+1, -y+2, -z+1	-9.7	-2.6	-18.6	10.7	-20.2	C27-H27···F4	3.356(4)/2.63/124
								(C26) π···π (C26)	3.478(4)
6 (M2···M1)	8.591	-x+1/2+1, +y-1/2, -z+1/2+1	-8.1	-1.9	-13.5	6.3	-17.2	C12-H12···F6	3.357(4)/2.79/113
								F2···π (C17/C18)	3.163(4)/3.105(4)
7 (M2···M1)	12.486	x+1/2, -y+1/2, +z+1/2	-11.3	-4.1	-11.8	10.7	-16.5	C3-H3···N4	3.429(4)/2.54/139
8 (M2···M2)	6.649	-x+1, -y+1, -z+1	-5.7	-1.7	-14.3	6.5	-15.2	C22-H22···F5	3.608(4)/2.62/153
								C22-H22···F6	3.584(3)/2.68/141
9 (M1···M1)	8.393	-x+1/2+1, +y-1/2, -z+1/2+1	-5.0	-2.3	-18.4	11.1	-14.6	C7-H7···F2	3.200(3)/2.51/120
10 (M1···M1)	13.389	x, +y+1, +z	-7.8	-1.6	-4.8	3.0	-11.2	C13-H13···N2	3.697(4)/2.68/156
11 (M2···M1)	7.521	-x+1/2+1, +y+1/2, -z+1/2+1	0.2	-1.8	-17.4	8.1	-10.9	C12-H12···F6	3.357(4)/2.79/113
								C27-H27···F3	3.454(4)/2.40/165
								F5···π (C2)	3.055(4)
12 (M2···M2)	13.389	x, y-1, z	-3.7	-1.5	-4.7	2.7	-7.2	N4···π (C28)	3.467(5)
4CN3T									
1 (M2···M1)	10.438	-x+1, -y+1, -z+1	-49.3	-17.7	-21.6	46.0	-42.6	N3-H3A···N2	3.136(4)/2.15/160
								C25-H25···N2	3.319(3)/2.26/166
								C21-H21···N2	3.370(3)/2.43/145
2 (M2···M1)	10.504	x, y, z	-39.1	-13.9	-18.2	33.3	-37.9	N1-H1···N4	3.070(4)/2.14/150
								C4-H4···N4	3.383(3)/2.67/123
								C10-H10···N4	3.377(3)/2.52/135
3 (M2···M2)	4.142	x, -y+1/2, +z+1/2	-8.3	-4.9	-57.3	34.3	-36.3	(C21)π···π(C18)	3.298(4)
4 (M1···M1)	3.834	x, -y+1/2, +z-1/2	-15.3	-7.5	-73.0	60.9	-34.8	(C6)π···π(C8)	3.440(4)
5 (M2···M1)	9.763	-x+1, -y, -z+1	-12.6	-5.1	-17.5	16.9	-18.2	C12-H12···O2	3.109(3)/2.36/126
								C13-H13···O2	3.226(4)/2.60/116
6 (M2···M1)	9.811	x-1, +y, +z-1	-8.1	-3.0	-14.8	9.6	-16.3	C27-H27···O1	3.371(3)/2.68/121
								C28-H28···O1	3.377(3)/2.71/120

								C7-H7···F8	3.191(3)/2.63/112
7 (M2···M1)	9.636	x, -y+1/2, +z-1/2	-8.1	-3.1	-10.0	5.2	-16.0	C22-H22···F6	3.683(3)/2.80//139
								C4-H4···N4	3.541(3)/2.68/136
8 (M2···M1)	9.160	x+1, -y+1/2, +z+1/2	-2.2	-2.0	-14.8	6.9	-12.2	C14-H14···F7	3.820(5)/2.82/154
								C14-H14···F8	3.519(3)/2.55/150
9 (M2···M1)	8.932	-x+1, +y+1/2, -z+1/2+1	-1.6	-1.2	-8.0	1.7	-9.1	C21-H21···F4	3.662(4)/2.91/127
4CN4T.F1									
1 (M2···M1)	5.049	x, y, z	-40.3	-17.4	-47.1	58.7	-46.1	C19-H19···O1	3.2271(3)/2.54/121
								N3-H3A···O1	2.8481(3)/1.87/156
								F5···π (C1)	3.0742(3)
2 (M2···M1)	4.984	x-1, y, z	-40.4	-17.5	-48.4	61.2	-45.2	N1-H1···O2	2.8468(3)/1.85/161
								C4-H4···O2	3.2423(2)/2.59/118
								F2···π (C16)	3.0499(2)
3 (M2···M1)	10.167	-x+2, -y, -z+2	-14.6	-5.2	-36.5	30.8	-25.6	C6-H6···N4	3.4877(2)/2.56/143
4 (M1···M1)	9.776	-x+1, -y, -z+1	-11.8	-4.5	-36.3	27.3	-25.2	(C6)π···π(C2)	3.3772(2)
5 (M2···M1)	6.914	-x+1, -y+1, -z+2	-4.4	-2.2	-28.6	14.4	-20.8	C25-H25···F1	3.3857(2)/2.35/160
								F3···π (C8)	3.1197(3)
								C25-H25···F3	3.5350(2)/2.74/131
6 (M2···M2)	6.960	-x+2, -y+1, -z+1	-3.2	-1.6	-25.8	11.5	-19.1	F4···π(C23/C25)	3.1920(3)/3.1852(3)
7 (M1···M1)	12.299	x, +y, +z-1	-7.2	-3.6	-13.8	8.4	-16.3	C3-H3···F2	3.5622(2)/2.55/155
								C13-H13···π (C1)	3.8068(2)/2.99/145
8 (M2···M2)	12.299	x, +y, +z+1	-7.2	-3.6	-13.8	8.4	-16.3	C18-H18···F5	3.5781(2)/2.58/153
								C28-H28···π (C16)	3.8262(2)/3.01/145
9 (M2···M1)	10.452	-x+2, -y, -z+1	-8.1	-3.2	-10.0	7.8	-13.6	C21-H21···N2	3.3446(2)/2.53/133
10 (M2···M1)	9.185	-x+1, -y+1, -z+1	-4.8	-2.2	-11.4	7.7	-10.7	C10-H10···F6	3.3677(2)/2.33/161
								C10-H10···F4	3.5544(2)/2.76/130
11 (M2···M1)	11.730	x+1, +y, +z-1	-1.4	-0.5	-5.1	2.1	-4.9	C28-H28···F2	3.3187(2)/2.64/120
								C30-F4···F1-C15	3.1455(3)/141, 131
4CN4T.F2									
1	4.166	-x+2, -y+1, -z+2	-17.3	-6.7	-62.2	45.9	-40.3	O1···π (C8)	3.031(4)
								C3-H3···F3	3.543(3)/2.73/132
2	11.188	x-1, -y+1/2, +z-1/2	-43.1	-15.8	-16.6	37.6	-37.9	N1-H1···N2	3.010(4)/2.03/158
								C6-H6···N2	3.469(4)/2.71/127
								C14-H14···N2	3.378(4)/2.75/117

3	6.465	-x+1, -y+1, -z+1	-0.9	-2.0	-33.7	16.5	-20.1	F1···π (C8)	3.160(4)
4	7.744	x-1, y, z	-9.6	-4.9	-17.7	14.6	-17.6	C13-H13···O1	3.304(4)/2.23/173
								C10-H10···F1	3.661(4)/2.59/173
5	10.737	-x+2, +y+1/2, -z+1/2+1	-2.4	-1.7	-8.3	4.5	-7.9	C11-H11···π (C1)	3.885(4)/2.94/154
								C11-H11···N2	3.830(4)/2.83/154
6	10.715	-x+1, +y-1/2, -z+1/2+1	-2.3	-0.8	-7.4	3.5	-7.0	C6-H6···F2	3.306(4)/2.70/115

3CN2T*				
Motif	Symmetry Code	E_{total}	Involved interactions	Geometry (Å/°)
1 (M3···M2)	x, y, z	-66.6	N5-H5A···O2	2.908(2)/1.91/162
			F4···π(C35)	3.073/129
			(C28) π···π (C31)	3.338
2 (M2···M1)	x, y, z	-62.0	N3-H3A···O1	3.026(2)/2.00/176
			C20-H20···π(C9/C14)	3.539(1)/2.66/166
				3.393(1)/2.69/159
			F2···F5	2.705(1)/163, 108
3 (M1···M3)	x, +y, +z-1	-57.0	N1-H1···O3	2.860(2)/1.86/164
			C5-H5···O3	3.404(2)/2.61/130
			(C41) π···π (C12)	3.366(3)
			F7···π(C10)	3.038(2)/131
4 (M3···M3)	-x+1, -y+1, -z+2	-39.4	C34-H34···O3	3.447(3)/2.39/167
			C34-H34···F7	3.353(2)/2.65/122
			C34-H34···F8	3.345(2)/2.69/119
			C33-H33···F7	3.352(2)/2.66/122
5 (M3···M2)	-x+1, -y, -z+2	-22.4	C41-H41···O2	3.880(2)/2.82/169
			C41-H41···F5	3.376(2)/2.70/120
			C42-H42···F4	3.588(2)/2.64/146
			F9···π (C22/C17/C16)	2.945(2)/3.096(2)/2.970(2)
6 (M2···M1)	-x+1, -y, -z+1	-20.7	C12-H12···F5	3.384(2)/2.51/137
			F3···π(C19)	3.171(2)
7 (M2···M1)	-x+1, -y+1, -z+1	-20.6	C26-H26···F1	3.197(2)/2.47/124
			F6···π(C7/C2/C1)	3.219(3)/3.204(2)/3.175(2)
8 (M3···M2)	-x, -y, -z+2	-17.4	C44-H44···N4	3.661(3)/2.70/148
9 (M3···M2)	x, +y-1, +z	-17.1	C18-H18···N6	3.585(2)/2.55/161
10	-x+1, -y, -z+1	-15.4	C11-H11···F2	3.533(2)/2.79/126

(M1···M1)				
11 (M1···M3)	-x, -y+1, -z+1	-14.7	C14-H14···N6	3.711(2)/2.89/133
12 (M1···M2)	x, +y+1, +z-1	-14.7	C4-H4···N4	3.458(2)/2.56/140
13 (M2···M2)	-x, -y, -z+2	-11.5	C22-H22···N4	3.442(2)/2.63/129
14 (M2···M1)	x, +y-1, +z	-10.5	C19-H19···N2	3.849(3)/2.82/159

* The interaction energy of 3CN2T was calculated using *Crystal Explorer 21.5*.

	N	Symop	R	Electron Density	E_ele	E_pol	E_dis	E_rep	E_tot
	0	-	4.90	B3LYP/6-31G(d,p)	-42.3	-10.4	-55.6	62.9	-62.0
	1	-	4.90	B3LYP/6-31G(d,p)	-45.7	-10.2	-50.4	53.6	-66.6
	1	-	9.40	B3LYP/6-31G(d,p)	1.3	-0.4	-1.4	0.0	-0.2
	0	-	11.00	B3LYP/6-31G(d,p)	-1.4	0.0	-11.9	8.4	-6.7
	0	-x, -y, -z	7.40	B3LYP/6-31G(d,p)	-13.6	0.0	-16.6	5.8	-25.3
	0	-	7.62	B3LYP/6-31G(d,p)	-11.4	0.0	-37.0	22.5	-30.4
	1	-	10.03	B3LYP/6-31G(d,p)	-13.1	-4.0	-11.5	6.4	-22.9
	0	-	8.38	B3LYP/6-31G(d,p)	-5.7	-1.0	-14.6	6.5	-15.4
	0	-x, -y, -z	10.07	B3LYP/6-31G(d,p)	-7.2	-1.5	-19.7	8.3	-20.7
	0	x, y, z	13.16	B3LYP/6-31G(d,p)	-1.1	-1.4	-4.8	0.0	-6.4
	1	-	4.89	B3LYP/6-31G(d,p)	-37.9	-11.6	-57.7	68.0	-57.0
	0	-	14.62	B3LYP/6-31G(d,p)	2.5	-0.2	-0.9	0.0	1.7
	1	-	7.25	B3LYP/6-31G(d,p)	-1.0	-1.1	-13.3	1.5	-12.4
	0	-	13.05	B3LYP/6-31G(d,p)	-8.3	-2.5	-4.8	0.0	-14.7
	0	-	7.85	B3LYP/6-31G(d,p)	-6.2	-1.2	-22.8	10.7	-20.6
	1	-	12.25	B3LYP/6-31G(d,p)	3.2	-1.0	-8.3	0.0	-4.5
	0	-	13.45	B3LYP/6-31G(d,p)	-6.6	-1.7	-2.7	0.0	-10.5
	1	-	12.18	B3LYP/6-31G(d,p)	-2.5	-2.8	-14.1	0.0	-17.1
	1	-	9.93	B3LYP/6-31G(d,p)	-9.9	0.0	-17.4	13.2	-17.4
	0	-x, -y, -z	10.01	B3LYP/6-31G(d,p)	-6.6	0.0	-13.6	11.9	-11.5
	0	-x, -y, -z	12.49	B3LYP/6-31G(d,p)	1.5	-0.3	-1.8	0.0	-0.3
	1	-	7.93	B3LYP/6-31G(d,p)	-8.7	-1.9	-25.1	16.4	-22.4
	0	x, y, z	13.16	B3LYP/6-31G(d,p)	4.0	-0.4	-2.3	0.0	1.9
	0	-x, -y, -z	9.74	B3LYP/6-31G(d,p)	-2.5	-0.6	-15.5	7.2	-12.2
	1	-x, -y, -z	8.97	B3LYP/6-31G(d,p)	-0.8	0.0	-28.3	18.4	-14.1
	1	-x, -y, -z	7.60	B3LYP/6-31G(d,p)	-4.4	-1.2	-44.8	29.9	-26.1
	1	-x, -y, -z	6.88	B3LYP/6-31G(d,p)	-25.6	-0.3	-35.8	30.7	-39.4

Figure S6: Energy decomposition into electrostatic, polarization, dispersion, and repulsion components for 3CN2T via *Crystal Explorer 21.5*. Values mentioned in the light green shade were considered in the total interaction energy topology for particular interactions.

S4. Hirshfeld surface analysis and 2D-Finger print plot:

A surface was generated for molecules in the asymmetric unit for substituted *N*-phenyl benzamides with the help of the 'Hirshfeld surface generation' option in *Crystal Explorer 21.5* (**Fig 14 in main manuscript**). Based on the surface generated, the % contribution of contacts is extracted using thefingerprint plots (**Fig. S5, Table 5**).

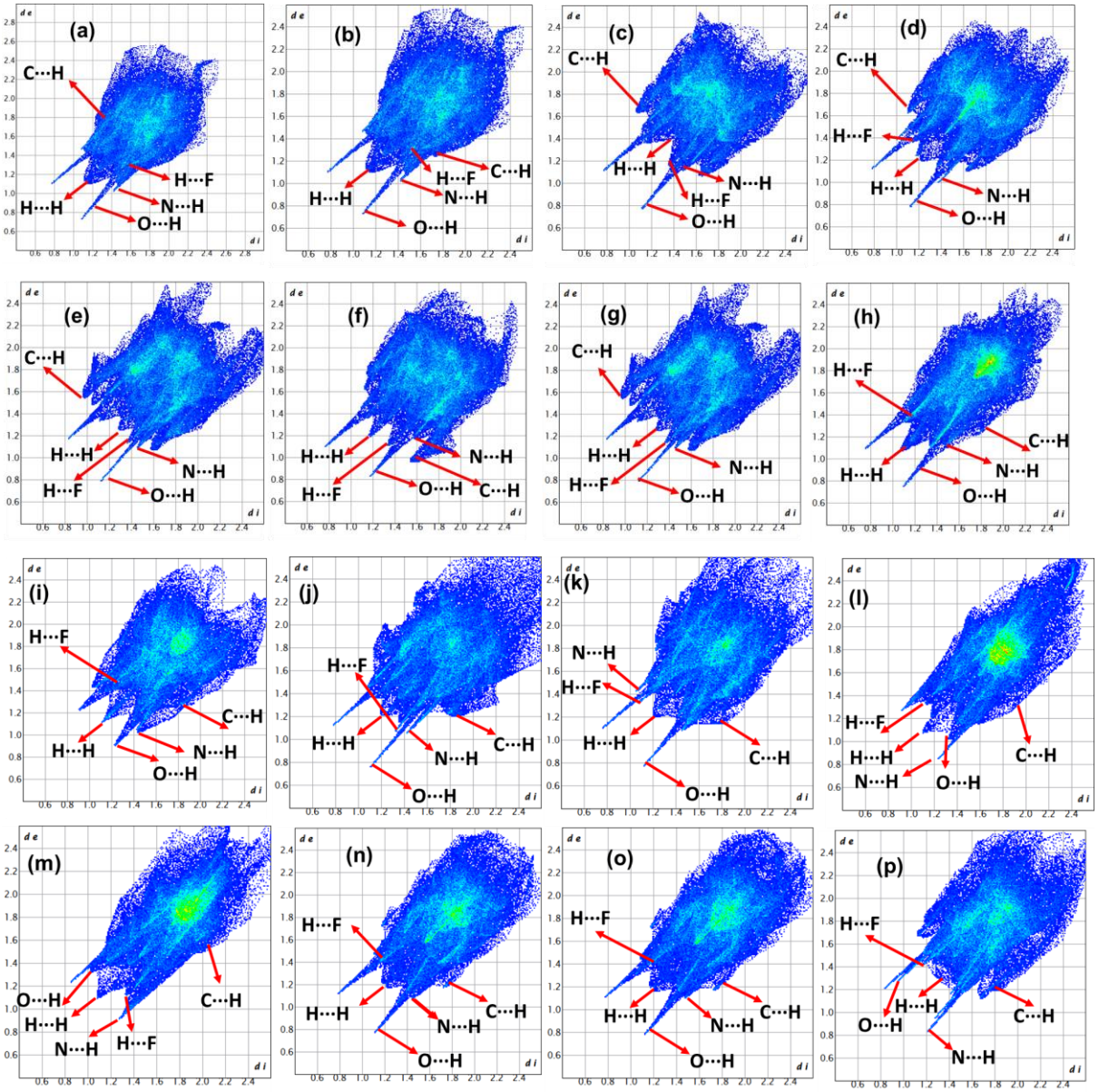

Figure S7: 2D- Fingerprint plot showing different intermolecular contact (red arrow) for (a, b) for 2CN2T.M1 and 2CN2T.M2, (c) 2CN3T, (d) 2CN4T, (e, f, g) 3CN2T.M1, 3CN2T.M2, and 3CN2T.M3, (h) 3CN3T, (i) 3CN4T, (j, k) for 4CN2T.M1, and 4CN2T.M2, (l, m) for Compound 4CN3T.M1, and 4CN3T.M2, (n, o) for 4CN4T.F1.M1, and 4CN4T.F1.M2, and (p) for 4CN4T.F2.

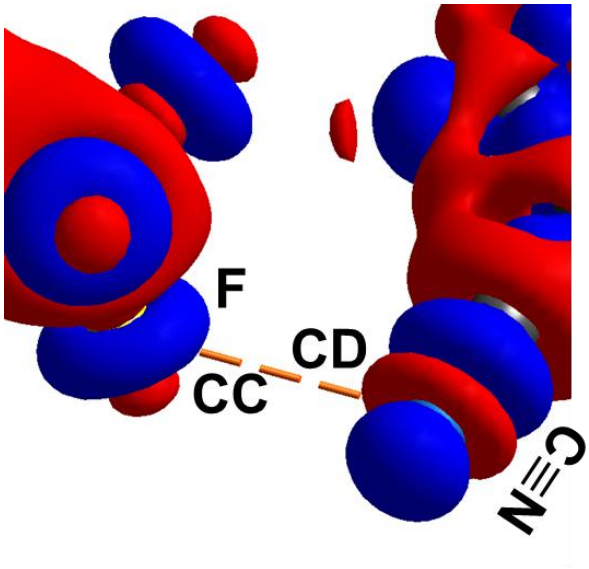

Figure S8: 3D-deformation density plot for F···π (-C≡N) interactions showing CC region (blue) of a fluorine atom and CD region (red) of -C≡N group for 3CN4T.

S5. Lattice energy

Computation of Lattice energy using PixelC: The total interaction energy is the combination of coulombic, polarization, dispersion, and repulsion contributions. The electron densities are calculated at the MP2/6-31G (d,p) level for all substituted *N*-phenyl benzamides using GAUSSIAN09 (Frisch, 2009). The MLC files, which are generated after calculations, provide the computed values of the lattice energies (**Table 4**).

Computation of Lattice energy using Crystal Explorer 21.5: The lattice energy of substituted *N*-phenyl benzamides is computed with the help of *Crystal Explorer 21.5*. For one molecule in the asymmetric unit, a cluster of 20Å is created around the selected molecule, and the molecular fragments are completed. Further, the energy is computed for the cluster with the help of an accurate method constituting of B3LYP/6-31G (d, p). The energy is calculated by summing half of the product of N and E_{tot}. For $Z'>1$ molecule in the asymmetric unit, a cluster of 20Å is created around the selected molecule, and the molecular fragments are completed. The average value obtained for the individual molecule selected is tabulated in **Table 3** in the main manuscript.

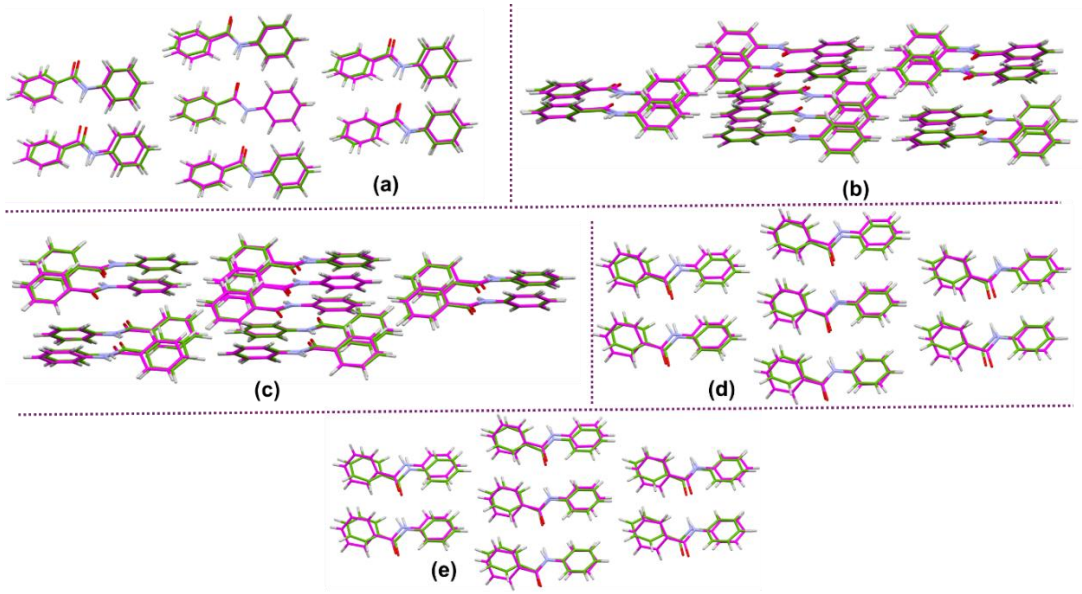

Figure S9: Overlay diagram of *N*-phenyl benzamide with (a) 2nd ranked structure depicting 7 out of 15 (to check) molecules with RMS value of 0.494 Å, (b) 5th ranked structure depicting 11 out of 15 molecules with RMS value of 0.255 Å, (c) 8th ranked structure depicting 11 out of 15 molecules with RMS values of 0.258 Å, (d) 23rd ranked structure depicting 7 out of 15 molecules with a RMS values of 0.780 Å and (e) 42nd ranked structure depicting 7 out of 15 molecules with a RMS values of 0.901 Å. In all cases, the magenta color represents predicted ranked structures.

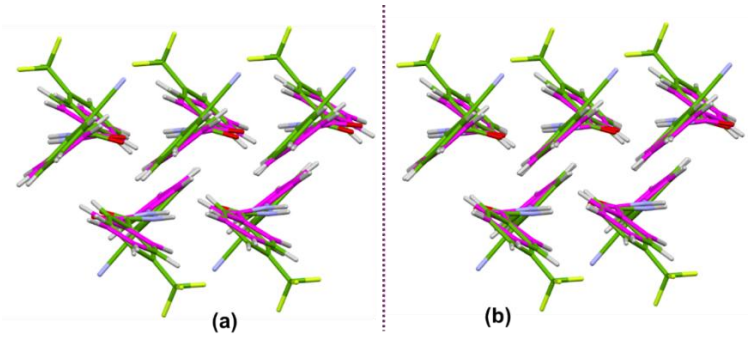

Figure S10: Overlay diagram of 2CN3T with (a) 27th ranked structure depicting 5 out of 15 molecules with RMS values of 0.282Å, (b) 36th ranked structure depicting 5 out of 15 molecules with an RMS value of 0.209 Å. In both cases, the magenta color represents predicted ranked structures.

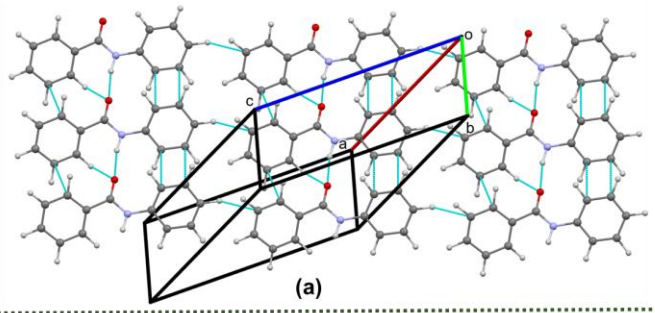

(a)

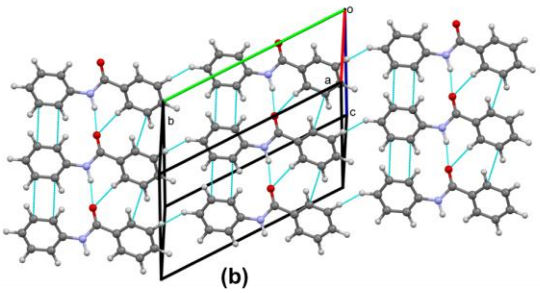

(b)

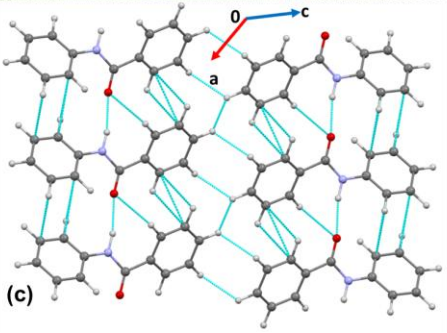

(c)

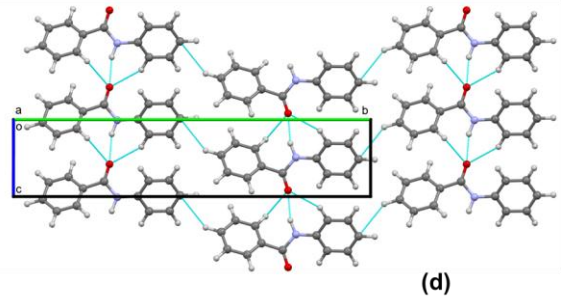

(d)

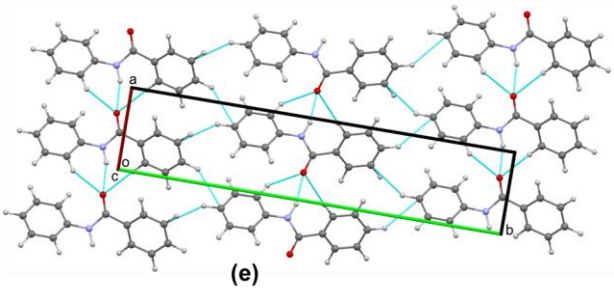

(e)

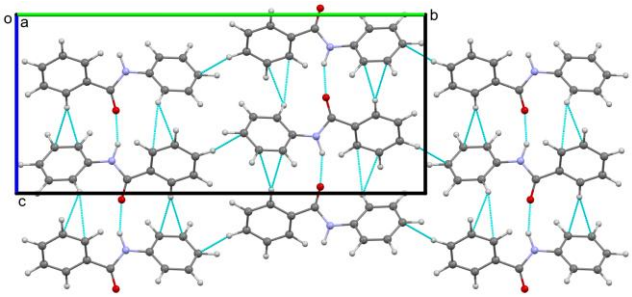

(f)

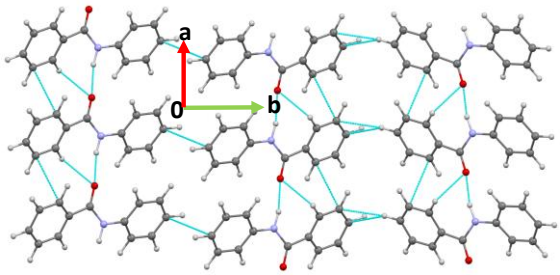

(g)

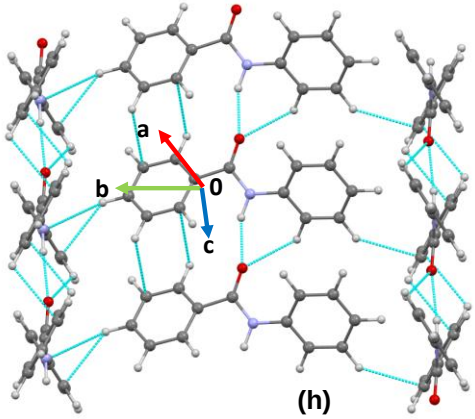

(h)

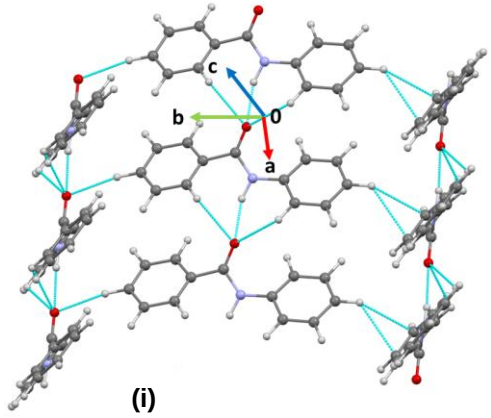

(i)

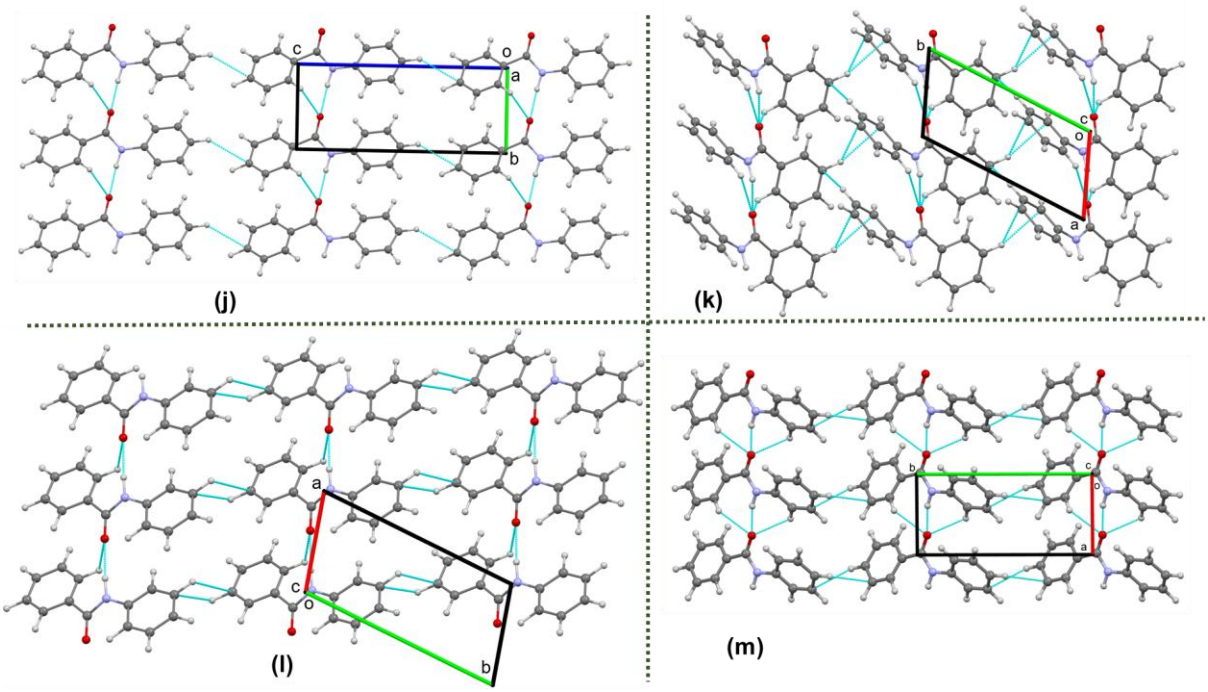

Figure S11: Crystal packing, depicting N-H/C-H···O, C-H··π/H interactions for the predicted (a)13th, (b) 85th, (c) 37th, (d) 4th, (e) 9th, (f)75th, (g) 87th, (h) 21st, (i) 24th, (j) 90th, (k) 31st, (l) 83rd , and (m) 97th ranked structures.

S6. Polymorph prediction:

Table S4: Prediction of the Top 100 polymorphs for the unsubstituted *N*-phenyl benzamide. The ranks highlighted in bold indicates the matching between hypothetical and experimental crystal structures based on similar unit cell types and space groups.

Rank	Space group	Cell volume	Density	Total Energy	Length a	Length b	Length c	Angle alpha	Angle beta	Angle gamma
1	*P*-1	474.71	1.380	-170.67	12.3458	9.4049	5.2172	57.684	78.890	68.016
2	***P*-1**	**482.49**	**1.358**	**-169.92**	**11.9036**	**8.4439**	**5.1158**	**87.681**	**75.191**	**76.119**
3	*P*-1	484.72	1.3518	-169.54	14.8128	5.1224	11.4624	87.905	139.524	111.086
4	***P*2$_1$/*c***	**968.40**	**1.353**	**-169.44**	**7.7728**	**24.0382**	**9.3943**	**90**	**146.515**	**90**
5	***P*-1**	**482.31**	**1.358**	**-169.34**	**7.71439**	**5.1924**	**12.3201**	**101.978**	**87.771**	**89.457**
6	*P*-1	484.52	1.352	-167.84	14.7190	9.3613	5.1757	57.254	86.162	58.073
7	*P*2$_1$/*c*	966.11	1.356	-167.84	14.1050	5.0981	24.8807	90	147.318	90
8	***P*-1**	**484.48**	**1.352**	**-167.63**	**5.1543**	**7.7674**	**12.3717**	**92.896**	**78.462**	**89.003**
9	***P*2$_1$/*c***	**972.41**	**1.347**	**-167.30**	**9.3194**	**24.2894**	**7.7461**	**90**	**146.319**	**90**
10	*P*2$_1$/*c*	991.25	1.322	-166.13	40.2201	5.1147	39.0087	90	172.904	90

11	*P*2$_1$/*c*	977.84	1.339	-166.01	12.5961	15.4248	5.1591	90	102.705	90
12	*P*-1	488.79	1.340	-166.02	5.0444	9.1901	13.1458	53.584	88.566	92.717
13	***P*-1**	**490.84**	**1.335**	**-165.92**	**11.2349**	**5.0562**	**12.5943**	**75.429**	**45.322**	**76.647**
14	*P*-1	495.24	1.323	-165.69	12.5700	9.9312	5.0336	86.994	74.157	55.690
15	*P*2$_1$/*c*	988.08	1.326	-165.67	14.2677	15.7606	5.1493	90	121.423	90
16	*P*2$_1$/*c*	979.05	1.338	-165.57	12.4744	15.5504	5.1758	90	102.889	90
17	*P*-1	493.02	1.329	-165.54	5.1181	8.5963	12.3066	106.255	101.161	100.758
18	*P*2$_1$/*c*	970.31	1.350	-165.43	5.2132	24.2695	13.0111	90	143.883	90
19	*P*-1	490.26	1.336	-165.11	5.0949	10.9786	9.0772	98.271	92.875	101.757
20	*P*2$_1$/*c*	988.20	1.326	-165.03	12.3873	16.2863	11.8915	90	155.675	90
21	***P*2$_1$/*c***	**990.76**	**1.322**	**-165.01**	**19.3361**	**13.4104**	**23.1382**	**90**	**170.495**	**90**
22	*P*2$_1$/*c*	979.79	1.337	-164.95	9.3587	24.6317	12.9367	90	160.819	90
23	***P*-1**	**491.39**	**1.333**	**-164.87**	**5.0888**	**8.3642**	**12.1489**	**106.017**	**82.549**	**87.879**
24	***P*2$_1$/*c***	**1000.00**	**1.309**	**-164.73**	**13.1764**	**18.5068**	**16.7233**	**90**	**165.804**	**90**
25	*P*2$_1$/*c*	988.82	1.325	-164.59	11.0498	17.7233	12.4485	90	156.071	90
26	*P*2$_1$/*c*	1000.00	1.309	-164.26	10.8201	19.9771	13.5605	90	160.046	90
27	***P*2$_1$/*c***	**1010.00**	**1.302**	**-164.21**	**5.0966**	**13.5171**	**16.9269**	**90**	**120.396**	**90**
28	*P*2$_1$/*c*	988.83	1.325	-164.12	42.5778	4.8314	41.1348	90	173.289	90
29	***P*2$_1$/*c***	**987.47**	**1.327**	**-164.09**	**5.1557**	**29.8708**	**7.05833**	**90**	**114.711**	**90**
30	*P*-1	499.84	1.310	-164.05	12.3636	5.0315	10.2039	95.488	124.995	99.030
31	***P*-1**	**495.62**	**1.321**	**-163.98**	**5.1211**	**9.5163**	**12.3059**	**99.471**	**113.472**	**107.620**
32	*P*2$_1$/*c*	980.52	1.336	-163.86	47.3747	5.0797	49.5078	90	175.279	90
33	*P*2$_1$/*c*	993.25	1.318	-163.84	38.4855	5.0460	38.1550	90	172.296	90
34	*P*-1	485.95	1.347	-163.81	5.0793	14.0874	9.4045	65.519	58.223	60.273
35	*P*-1	494.57	1.324	-163.77	5.0213	19.6720	5.0646	82.331	88.221	93.355
36	***P*2$_1$/*c***	**1000.00**	**1.304**	**-163.65**	**4.9829**	**17.7722**	**11.5129**	**90**	**99.748**	**90**
37	***P*2$_1$/*c***	**997.74**	**1.313**	**-163.63**	**12.0887**	**21.6909**	**9.4069**	**90**	**156.140**	**90**
38	*P*-1	1000.00	1.306	-163.39	22.4912	11.4783	19.5460	90	168.534	90
39	*P*-1	485.26	1.349	-163.38	5.3682	11.4559	9.1053	67.281	72.071	75.084
40	*P*-1	491.67	1.332	-163.36	6.7018	4.6487	23.8190	106.984	94.723	131.387

41	*P*-1	498.13	1.315	-163.31	5.0647	4.6502	25.1027	80.101	59.439	90.624
42	***P*-1**	**492.68**	**1.329**	**-163.30**	**5.1182**	**12.3166**	**8.3679**	**75.218**	**88.786**	**75.245**
43	*P*-1	497.468	1.317	-163.29	5.0380	16.3809	9.1098	70.499	57.019	52.074
44	$P2_1/c$	992.49	1.319	-163.21	10.4551	28.6434	7.2897	90	152.958	90
45	$P2_1/c$	971.2703	1.349	-163.19	4.1145	5.0669	46.5889	90	90.279	90
46	*P*-1	498.06	1.315	-163.06	5.0846	7.0441	24.7670	51.291	64.740	46.019
47	*P*-1	484.86	1.351	-162.99	5.0629	4.0937	24.9135	70.506	85.599	90.901
48	*P*-1	490.60	1.335	-162.98	8.8406	12.6854	5.1644	67.708	75.514	67.267
49	*P*-1	495.41	1.322	-162.94	4.6098	5.0769	21.2539	86.416	90.232	93.707
50	$P2_1/c$	985.30	1.329	-162.79	5.1010	4.4474	43.4316	90	89.796	90
51	$P2_1/c$	1010.00	1.301	-162.76	12.6520	17.4377	15.5344	90	162.912	90
52	*P*-1	485.79	1.348	-162.68	27.5083	4.0903	5.0715	89.060	66.575	69.603
53	*P*-1	499.77	1.311	-162.66	5.0476	4.6112	24.1558	76.134	67.369	91.2264
54	*P*-1	493.42	1.328	-162.56	4.4783	6.582	24.1213	66.483	81.147	49.9159
55	$P2_1/c$	1000.00	1.306	-162.55	6.9351	42.6191	5.0435	90	137.715	90
56	*P*-1	495.13	1.323	-162.54	23.6824	5.0842	4.5127	86.795	70.005	75.955
57	$P2_1/c$	1020.00	1.288	-162.49	5.0465	17.4586	11.5719	90	85.9472	90
58	$P2_1/c$	986.93	1.327	-162.49	4.4963	43.4559	6.6832	90	49.093	90
59	$P2_1/c$	1020.00	1.283	-162.49	5.0859	11.5459	19.9369	90	119.259	90
60	*P*-1	494.48	1.325	-162.48	6.6795	4.6425	24.3456	112.604	88.899	131.126
61	*P*-1	500.12	1.309	-162.45	4.6609	5.0680	22.0653	76.439	99.175	91.006
62	*P*-1	494.57	1.324	-162.31	22.8097	4.4618	5.05963	92.958	96.706	75.315
63	*P*-1	498.63	1.314	-162.16	4.6489	5.0761	22.1890	91.505	72.769	94.423
64	*P*-1	490.59	1.335	-161.93	10.3690	10.2472	5.2284	66.873	80.882	74.124
65	*P*-1	504.74	1.298	-161.85	13.0299	8.7225	5.1037	69.726	88.651	69.034
66	*P*-1	499.77	1.311	-161.84	12.813	8.1307	5.0504	96.799	104.267	97.204
67	*P*-1	501.86	1.305	-161.82	26.3765	6.9434	4.6255	46.618	58.599	57.1879
68	$P2_1/c$	1000.00	1.305	-161.79	5.1195	15.3608	13.6671	90	110.889	90
69	*P*-1	498.39	1.314	-161.74	25.8887	5.0826	4.5491	93.887	99.446	120.904
70	$P2_1/c$	1010.00	1.301	-161.72	6.9689	42.6556	5.0445	90	137.818	90

71	*P*-1	495.21	1.323	-161.63	4.4820	6.5647	23.5926	68.443	78.182	50.151
72	*P*-1	488.61	1.341	-161.52	28.3515	4.0833	5.0722	89.192	69.758	64.016
73	$P2_1/c$	1010.00	1.303	-161.46	4.6978	42.4080	10.3002	90	150.655	90
74	*P*-1	496.18	1.320	-161.40	27.2063	5.0677	4.4654	93.281	124.494	97.667
75	$\boldsymbol{P2_1/c}$	**990.26**	**1.323**	**-161.30**	**4.2513**	**22.9901**	**10.1534**	**90**	**86.264**	**90**
76	$P2_1/c$	1000.00	1.308	-161.30	4.5545	43.4032	5.0766	90	93.763	90
77	*P*-1	505.62	1.296	-161.29	13.8944	8.7639	5.0583	67.548	85.935	63.474
78	$P2_1/c$	1020.00	1.289	-161.18	11.7132	17.3066	13.5536	90	158.299	90
79	$P2_1/c$	1010.00	1.298	-161.17	9.4158	21.6047	9.7088	90	149.269	90
80	$P2_1/c$	1010.00	1.301	-161.05	12.4374	16.3128	14.5005	90	159.991	90
81	*P*-1	507.16	1.292	-161.03	12.6602	8.9714	5.0585	71.263	87.530	69.245
82	*P*-1	495.09	1.323	-161.02	7.0178	5.1526	17.3096	120.128	77.333	113.831
83	***P*-1**	**499.49**	**1.311**	**-161.01**	**5.0503**	**10.5078**	**10.0374**	**102.573**	**91.518**	**105.289**
84	*P*-1	499.92	1.310	-160.98	12.7547	9.1304	5.1473	64.730	81.773	67.302
85	***P*-1**	**500.53**	**1.309**	**-160.81**	**5.0571**	**14.1168**	**10.6601**	**73.823**	**49.541**	**60.050**
86	$P2_1/c$	974.25	1.345	-160.51	29.9516	10.3142	32.5698	90	174.444	90
87	$\boldsymbol{P2_1/c}$	**1000.00**	**1.305**	**-160.42**	**10.2151**	**43.9463**	**4.5404**	**90**	**150.458**	**90**
88	$P2_1/c$	989.88	1.323	-160.37	6.4531	47.4979	4.1357	90	128.659	90
89	***P*-1**	**505.19**	**1.297**	**-160.36**	**11.0650**	**5.0422**	**12.9507**	**93.359**	**123.278**	**115.06**
90	$\boldsymbol{P2_1/c}$	**1010.00**	**1.301**	**-160.07**	**15.9084**	**4.9749**	**20.2215**	**90**	**140.987**	**90**
91	$P2_1/c$	1020.00	1.286	-159.98	5.0074	40.2307	7.0656	90	45.712	90
92	*P*-1	498.67	1.314	-159.81	16.2523	5.1296	7.1263	67.547	67.653	90.943
93	$P2_1/c$	1000.00	1.306	-159.80	5.0645	16.7640	11.9013	90	96.895	90
94	*P*-1	506.38	1.294	-159.76	20.7609	5.0720	6.1432	67.006	59.614	86.324
95	$P2_1/c$	1010.00	1.291	-159.64	23.9983	4.4591	10.0880	90	109.982	90
96	$P2_1/c$	1030.00	1.277	-159.36	5.0581	43.8133	6.9612	90	138.329	90
97	***P*-1**	**522.09**	**1.255**	**-159.23**	**5.0593**	**11.3216**	**9.9318**	**70.717**	**76.489**	**85.966**
98	$P2_1/c$	1030.00	1.277	-159.20	5.0649	40.0020	7.0871	90	45.6202	90
99	$P2_1/c$	1030.00	1.277	-158.89	23.9641	5.0054	16.8860	90	149.561	90
100	$P2_1/c$	986.47	1.328	-158.71	15.5323	9.5898	9.8349	90	137.671	90

References:

Bruker, (2014). SADABS. Bruker AXS Inc., Madison, Wisconsin, USA.

Bruker, (2023). APEX5. Bruker AXS Inc., Madison, Wisconsin, USA**.**

Dance, I. (2003). *New J. Chem.* **27**, 22–27.

Degen, T., Sadki, M., Bron, E., König, U. & Nénert, G. (2014). *Powder Diffr.* **29**, S13–S18.

Dolomanov, O. V, Bourhis, L. J., Gildea, R. J., Howard, J. A. K. & Puschmann, H. (2009). *J. Appl. Crystallogr.* **42**, 339–341.

Frisch, M. (2009). *Inc, Wallingford CT* **201**.

Nardelli, M. (1995). *J. Appl. Crystallogr.* **28**, 659.

Petříček, V., Palatinus, L., Plášil, J. & Dušek, M. (2023). *Jana2020 – a new version of the crystallographic computing system Jana*. **238**, 271–282.

Sheldrick, G. M. (2008). *Acta Crystallogr. Sect. A Found. Crystallogr.* **64**, 112–122.

Sheldrick, G. M. (2015*a*). *Acta Crystallogr. Sect. C, Struct. Chem.* **71**, 3–8.

Sheldrick, G. M. (2015*b*). *Acta Crystallogr. Sect. A Found. Adv.* **71**, 3–8.

Spek, A. L. (2009). *Acta Crystallogr. Sect. D* **65**, 148–155.